Reminders of SAR basics. Discussion on Challenges of S1 for Fire Applications

Antonio Pepe

Istituto per il Rilevamento Elettromagnetico dell'Ambiente (IREA)
Consiglio Nazionale delle Ricerche (CNR)
Via Diocleziano, 328, 80124 Napoli (Italy)

Summary

- **Synthetic Aperture Radar Reminders**
- **SAR Data Processing**
- **Burned Areas Mapping Extraction**
- **Recent Literature on Fire Mapping Using SAR Data**

Radio Detection and Ranging (RADAR)

By exploiting electromagnetic wave signals (Radio), a RADAR system allows the detection of an object in space and to retrieve an information about the sensor-to-target distance (Ranging).

It works by measuring the time delay from the transmitted and the backscattered (received) signal onboard the sensor.

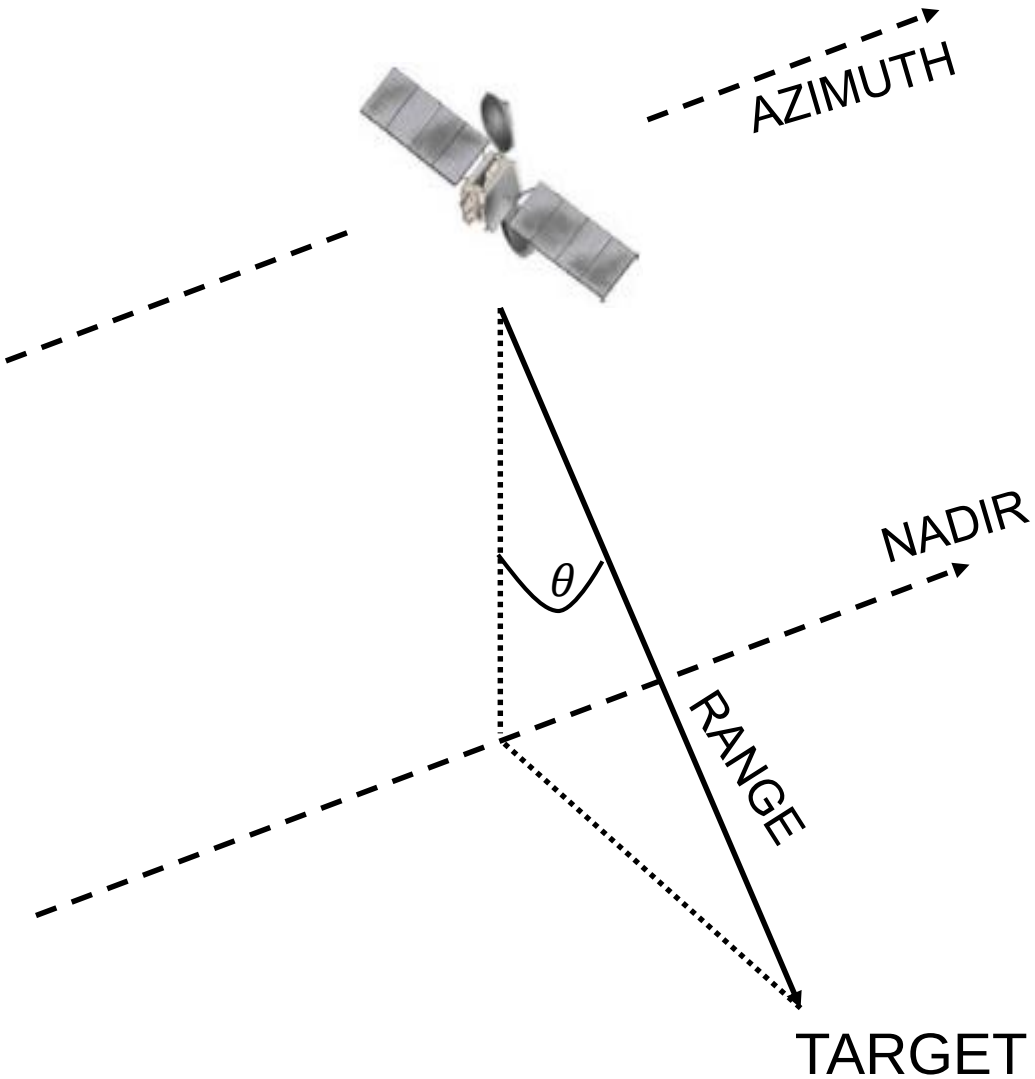

One more consideration about radar systems: the <u>roughness</u> of the imaged area plays a <u>fundamental role</u> due to the side-looking illumination scenario.

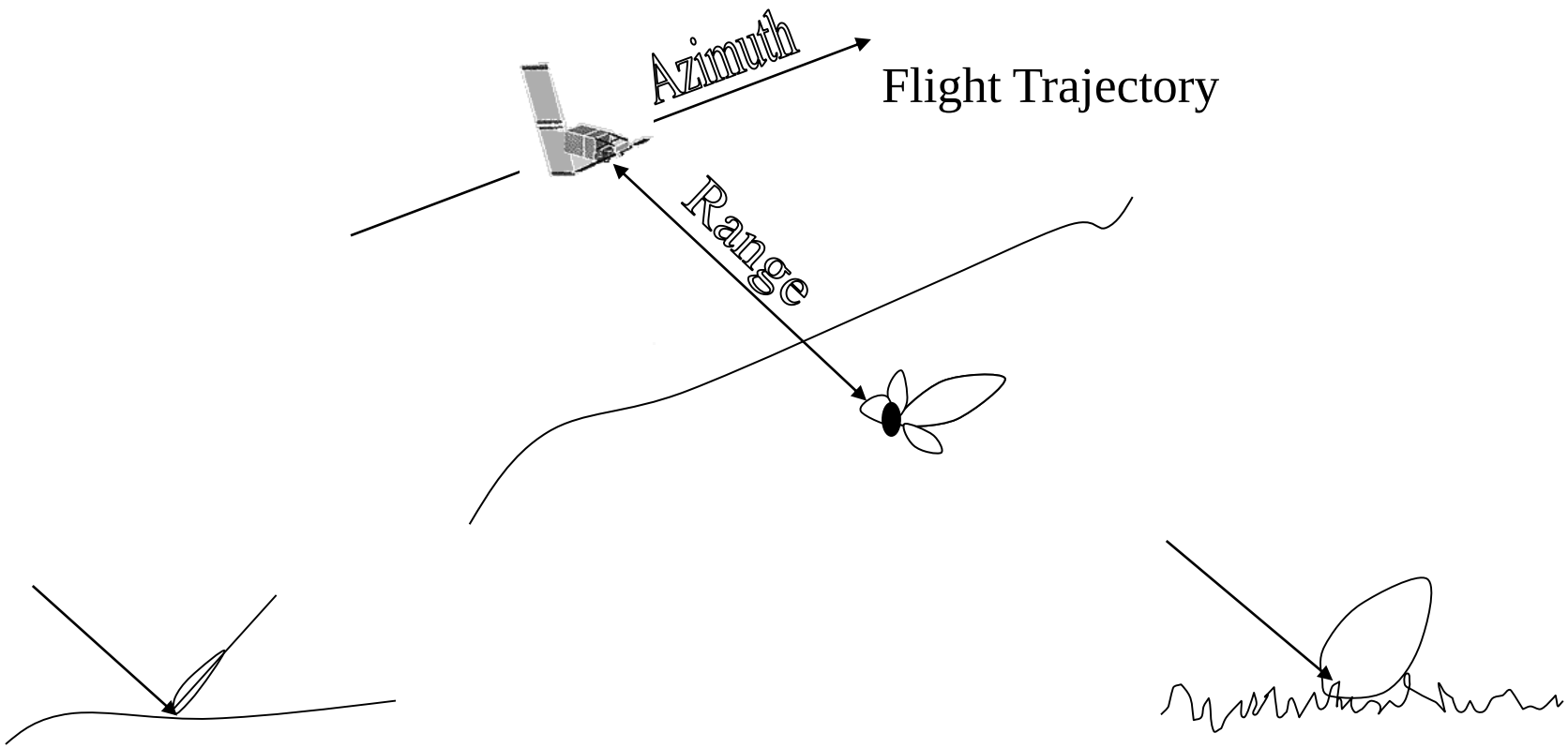

Flat scene
(no backscattered signal)

Rough scene
(backscattered signal)

Range Resolution

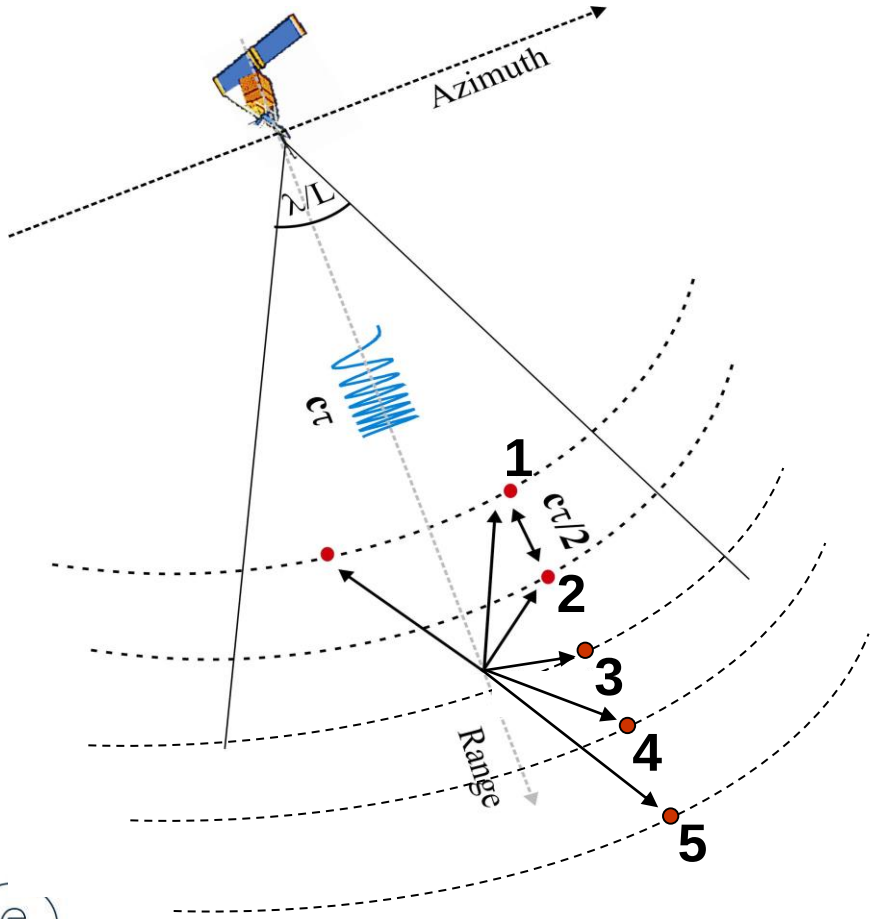

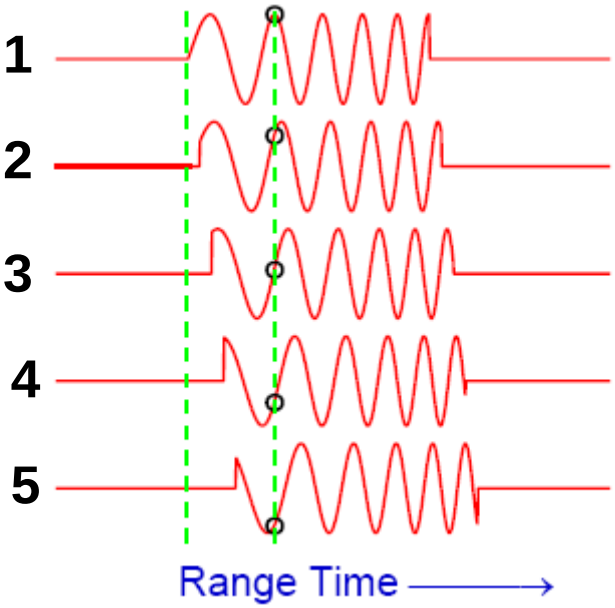

Azimuth Resolution

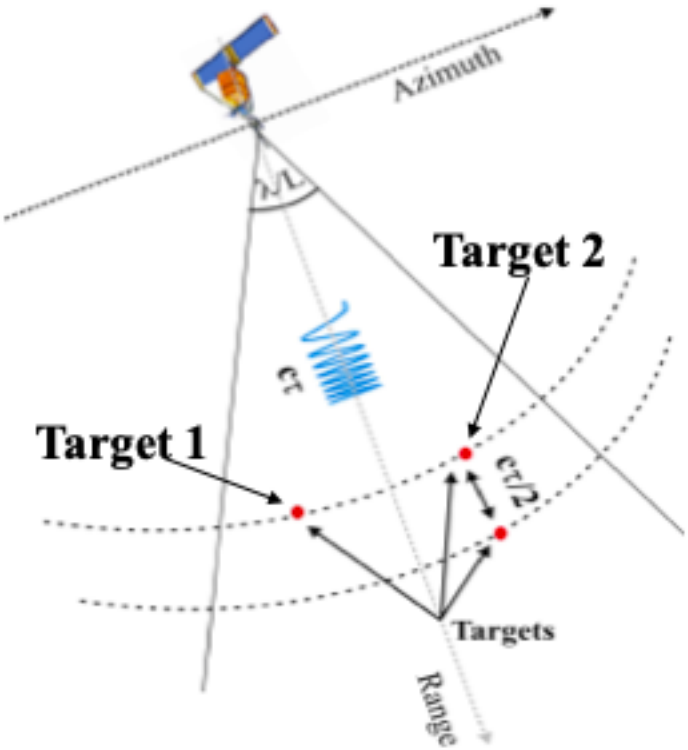

$$\Delta x \approx r \frac{\lambda}{L}$$

Targets 1 and 2 are not distinguished because they are to same distance from the sensor (range) and are illuminated by the same antenna beam (azimuth).

Concept of Synthetic Aperture

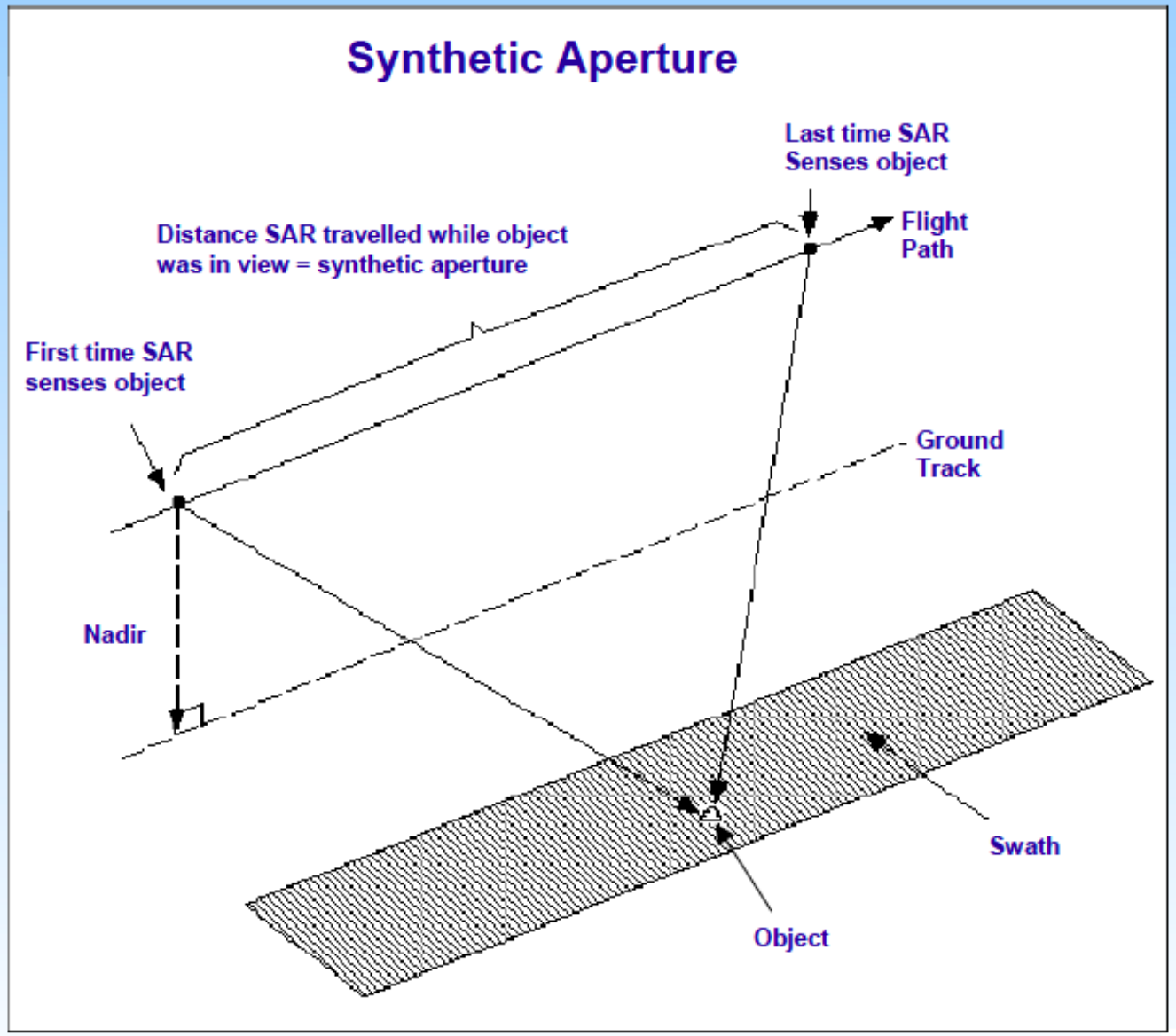

SAR Acquisition Modes

- STRIPMAP
- SPOTLIGHT
- ScanSAR (burst)
- TOPSAR

Stripmap mode

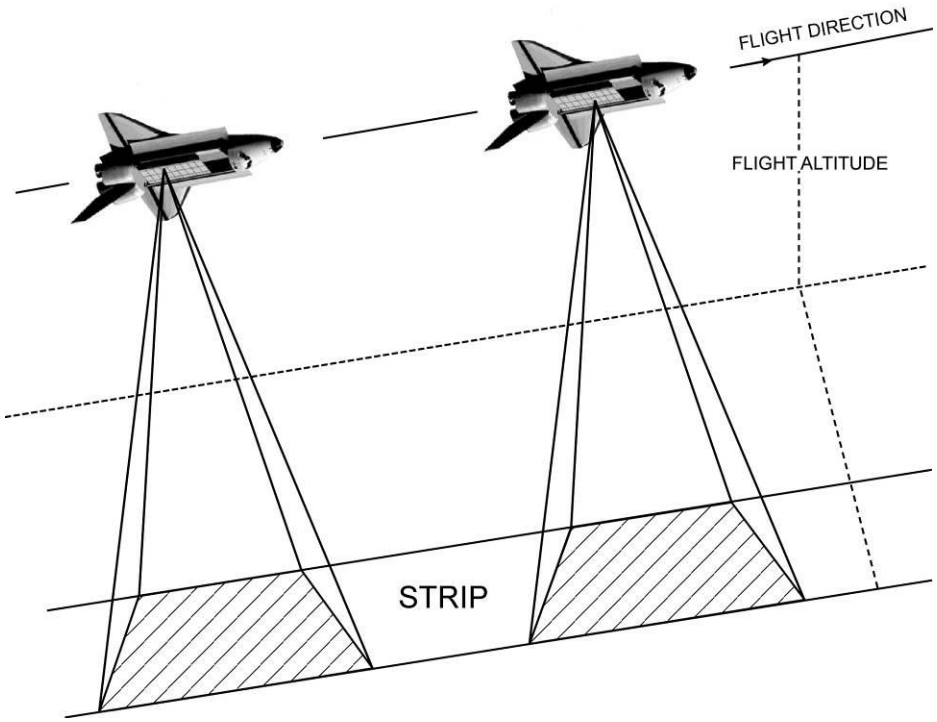

In this case the radar antenna points along a fixed direction with respect to the flight platform path and the antenna footprint covers a <u>strip</u> on the illuminated surface as the platform moves and the system operates. The SAR image dimension is limited in the across track (*range*) direction but, at least in principle, not in the along track (*azimuth*) one.

SAR image generation (data focusing) key steps: ERS example

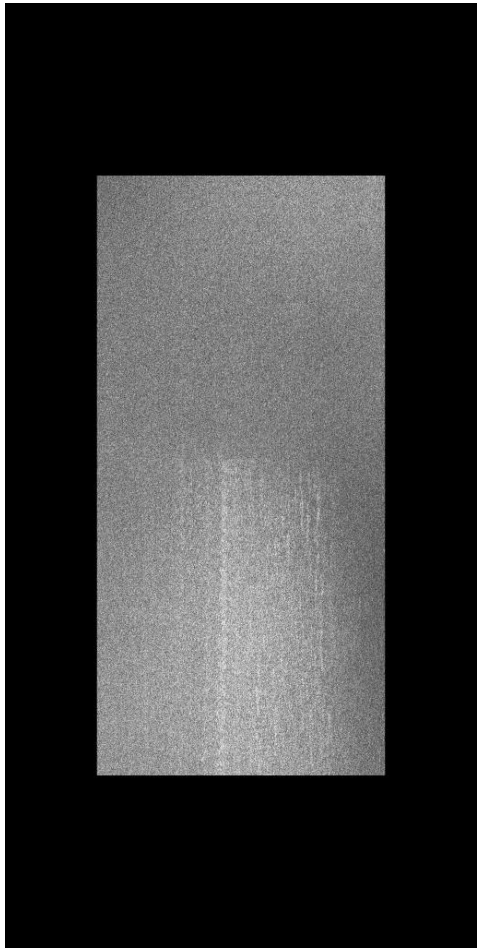

raw data

SAR image generation (data focusing) key steps: ERS example

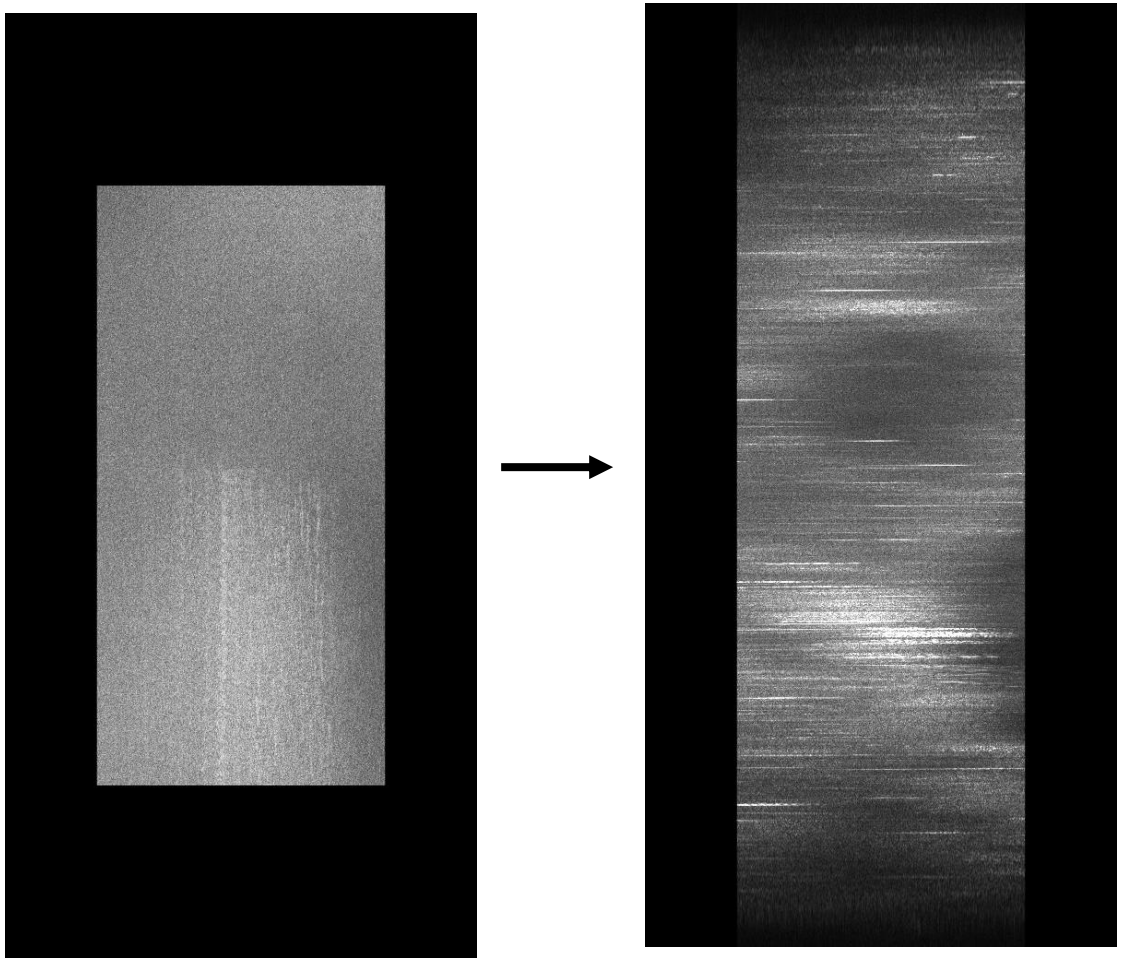

raw data **range compressed data**

SAR image generation (data focusing) key steps: ERS example

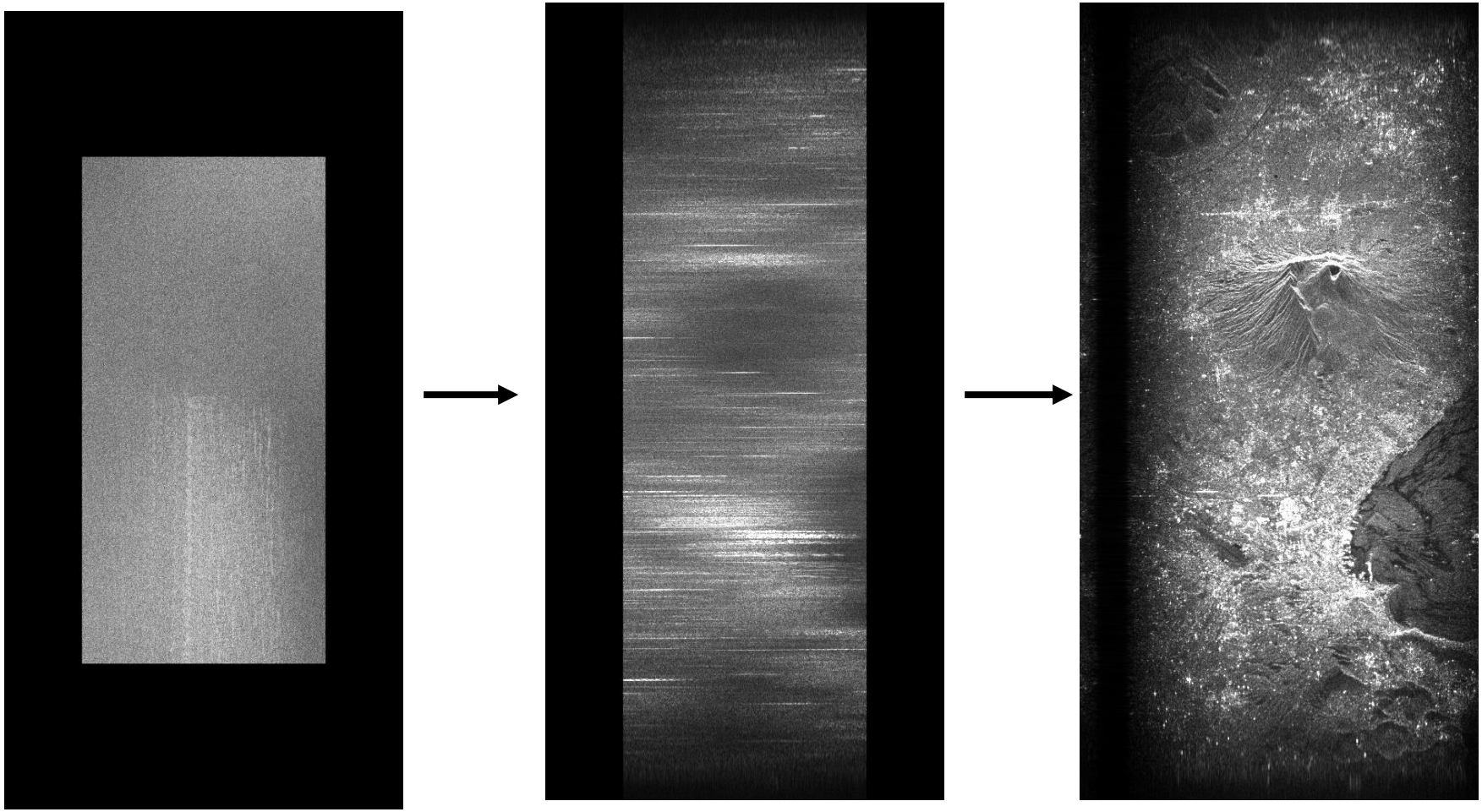

raw data **range compressed data** **focused image**

SAR Impulsive Response

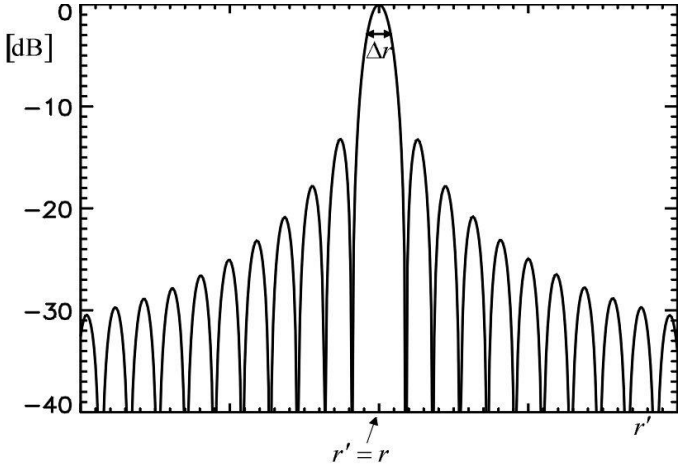

Range

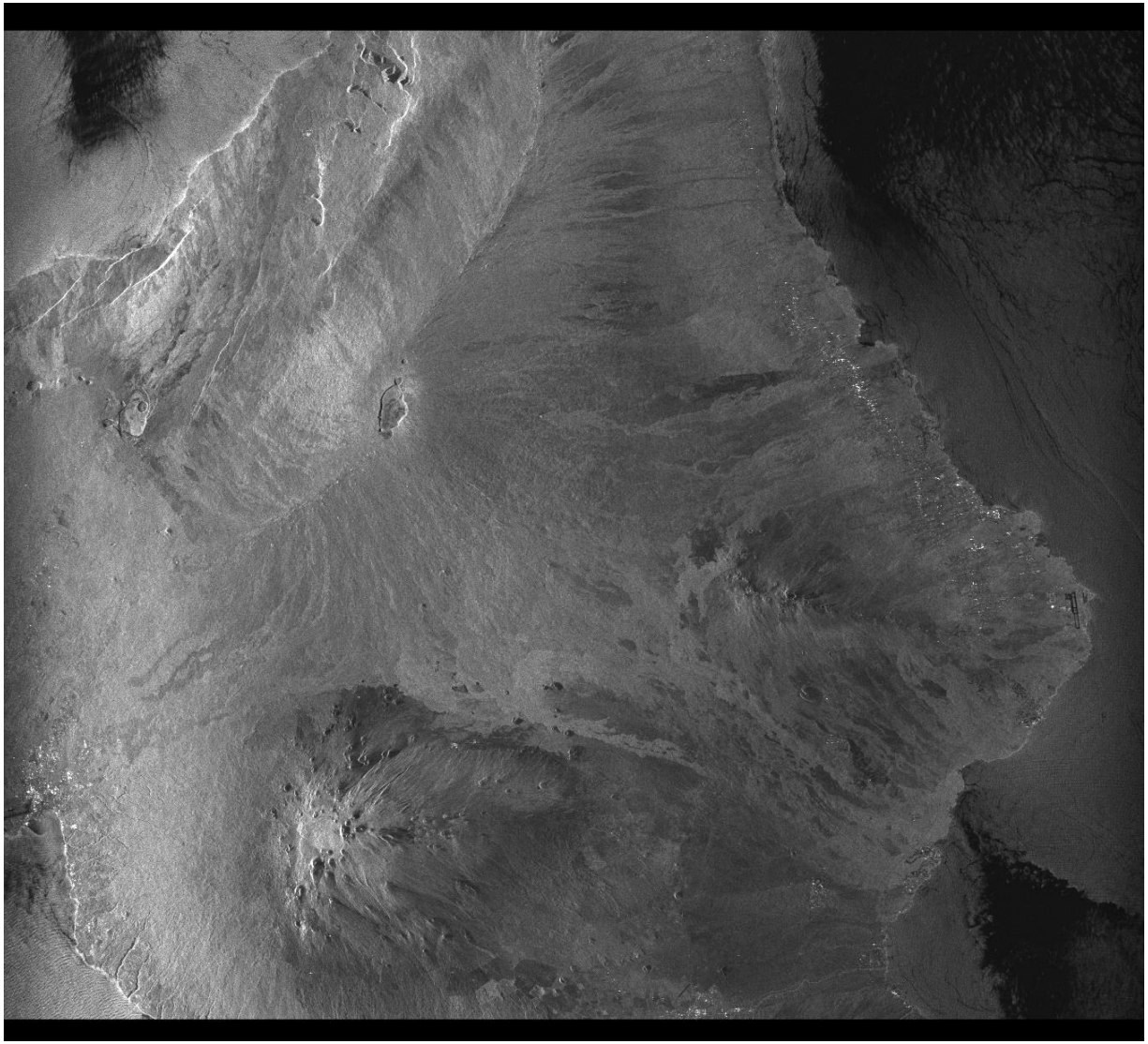

azimuth

range

StripMap

Spotlight mode

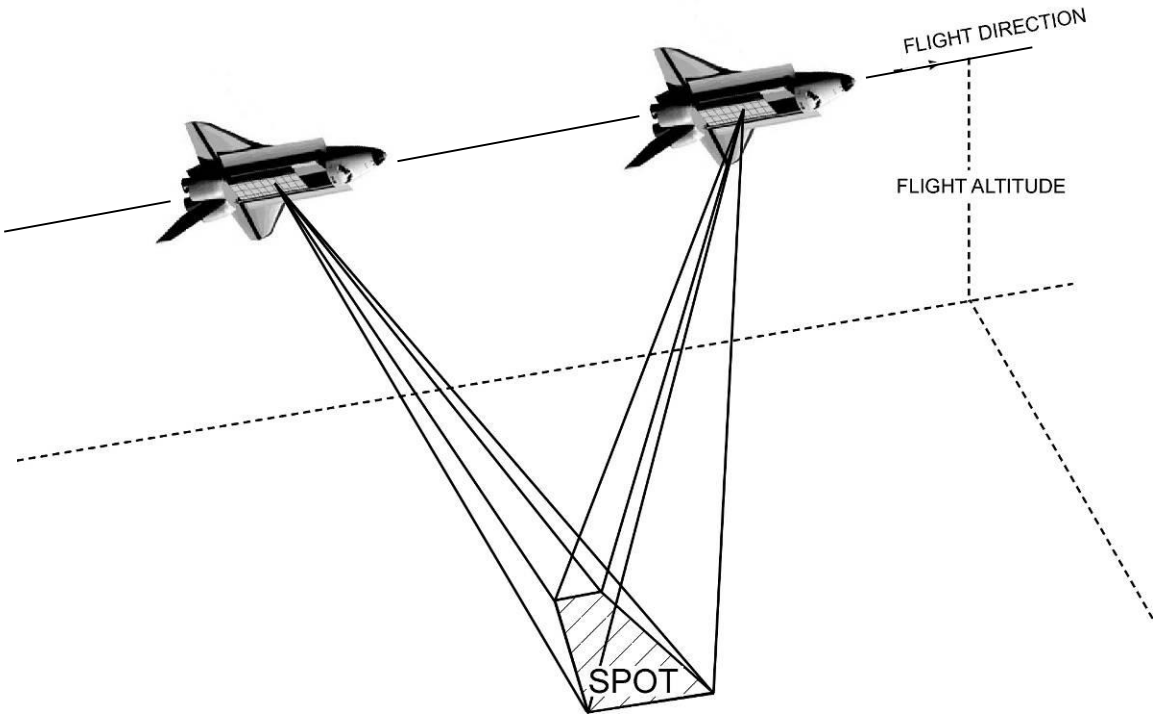

The radar antenna is steered during the overall acquisition time in order to illuminate the same area (*spot*) . The available synthetic antenna length can be increased with respect to the strip mode, thus improving azimuth resolution; this gain is traded off by loss of coverage due to the illumination of a limited area .

Spotlight Image (examples)

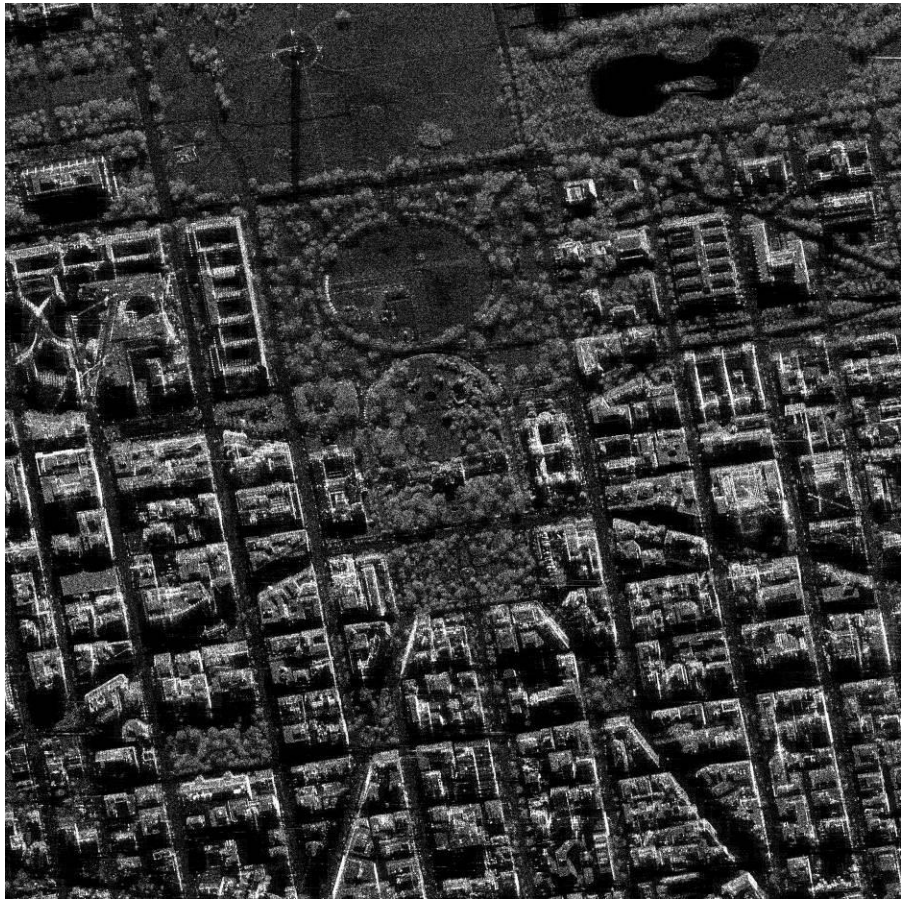

Ku-band (15 GHz) 1m x 1m resolution spot images of the White House, in Washington, D.C respectively (courtesy of Sandia National Lab.).

Ku-band (15 GHz) 1m x 1m resolution spot images of the Pentagon area, in Washington, D.C respectively (courtesy of Sandia National Lab.).

ScanSAR mode

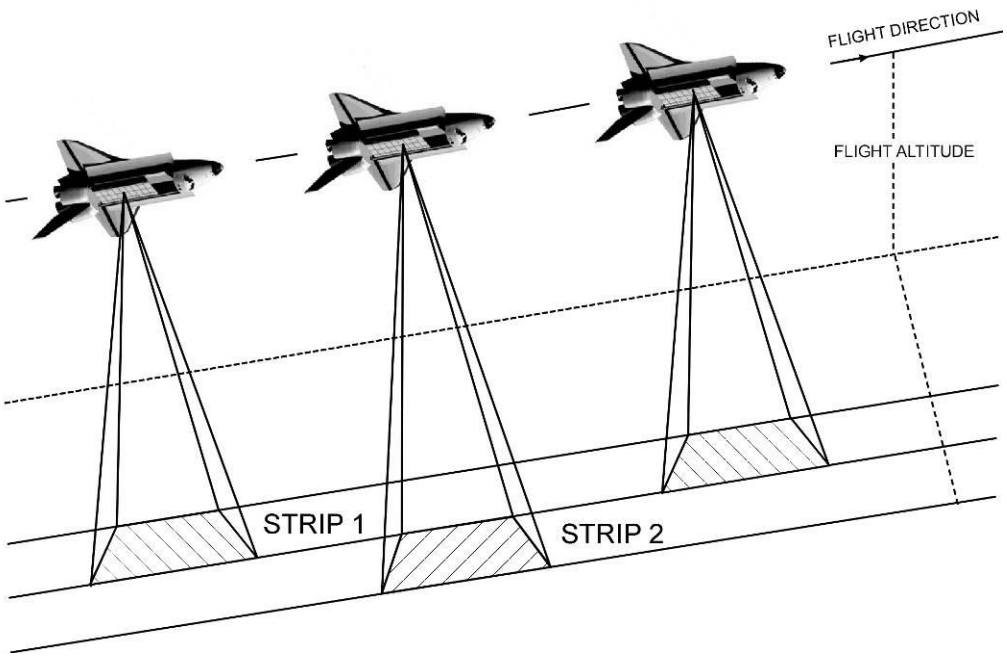

This mode allows a drastic <u>increase of the range swath dimension</u> by <u>periodically stepping the antenna beam to neighbouring subswaths</u> (in the range direction). In this case the range swath dimension increases at the expenses of azimuth resolution. In particular cases the system illuminates only one subswath but transmits burst signals (<u>burst mode</u>); <u>this allows us to reduce power consumption and data rates.</u>

ScanSAR and Burst Mode Data Processing

As already anticipated scanSAR and burst data processing is carried out by focusing each raw data burst individually, including the scalloping compensation and then incoherently combining the different burst images. In the scanSAR case the different subswath images may be combined to produce an overall image

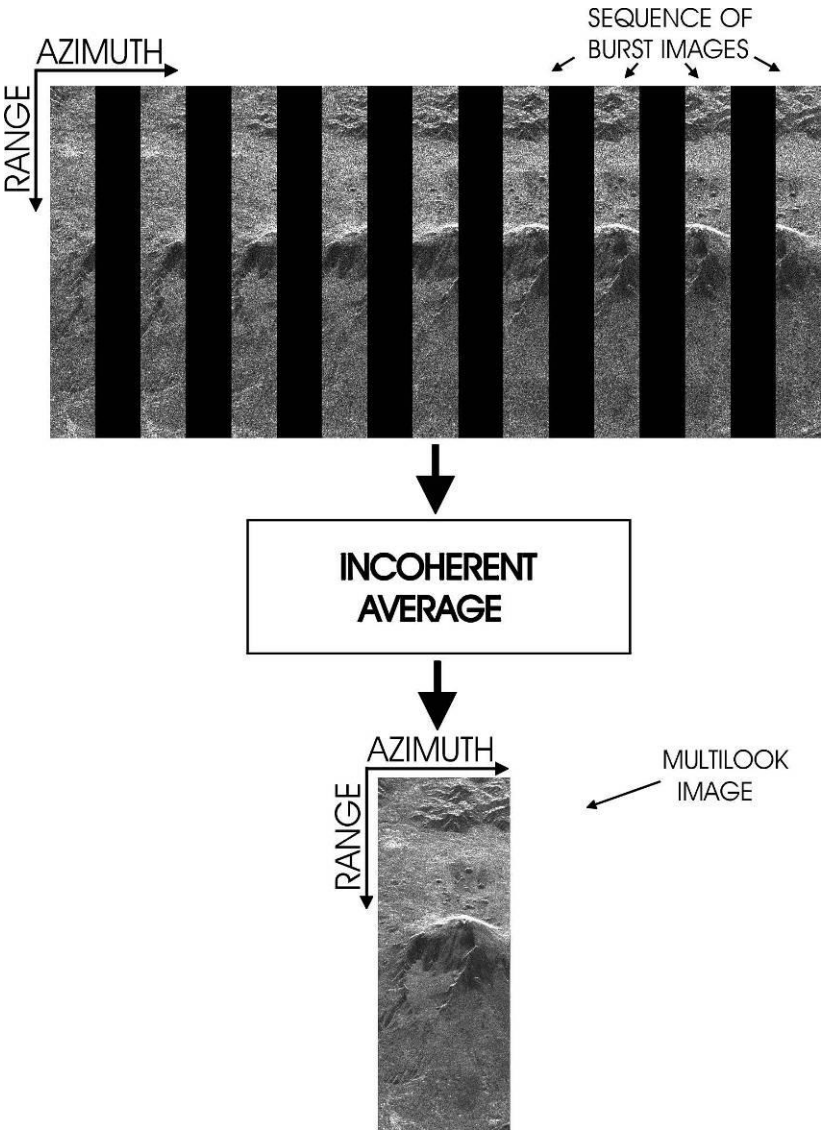

Scan Mode Analysis

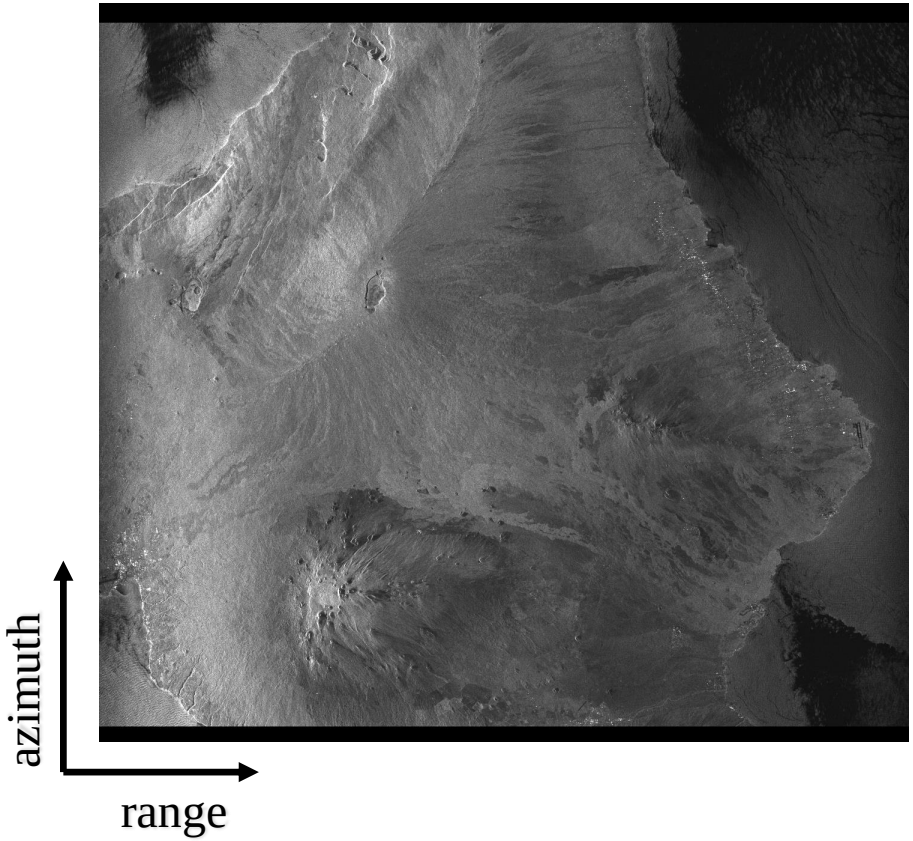

StripMap

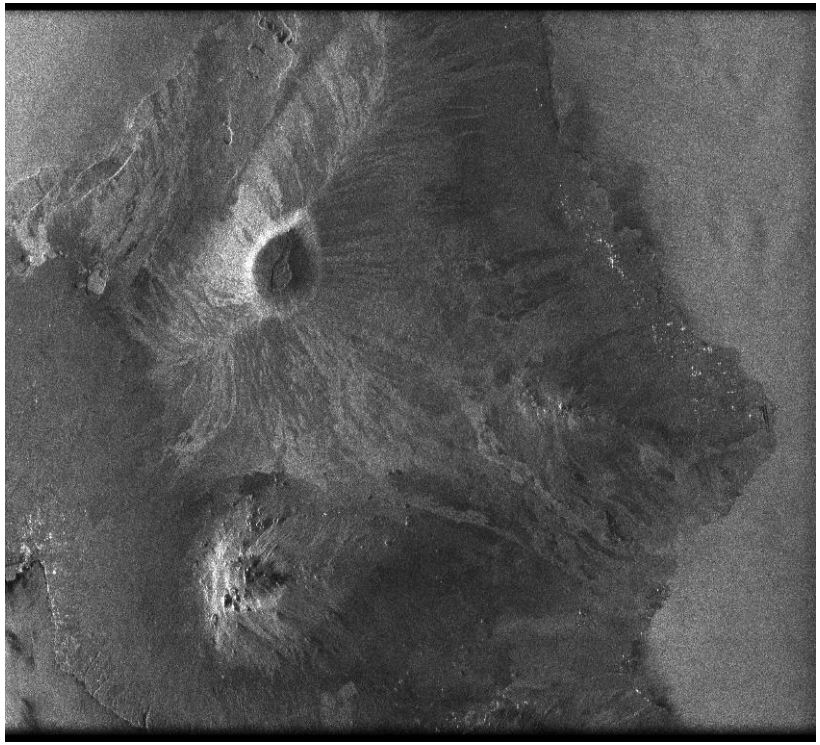

ScanSAR

Terrain Observation by Progressive Scan

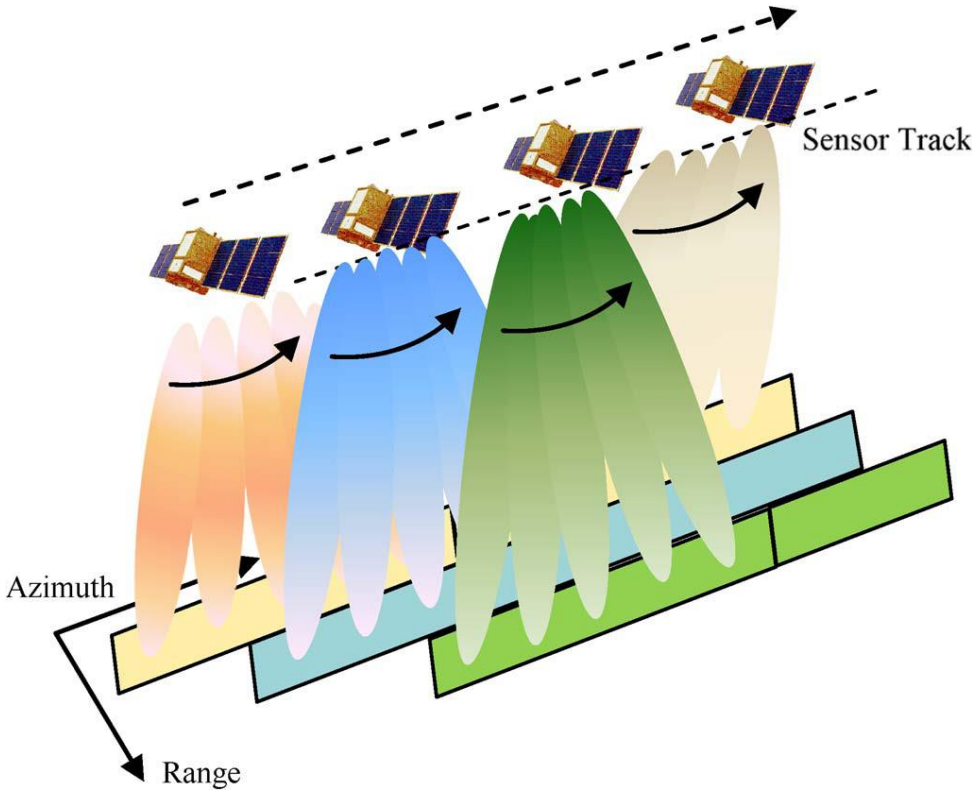

In the TOPS mode the antenna is rotated opposite with respect to SPOT. The sensor gathers the returns from a much longer strip with respect to the standard STRIPMAP mode within the same time span. It is going to be the operational mode for SENTINEL-1 Interferometric Wide Swath (IWS) mode.

esa

Bursting

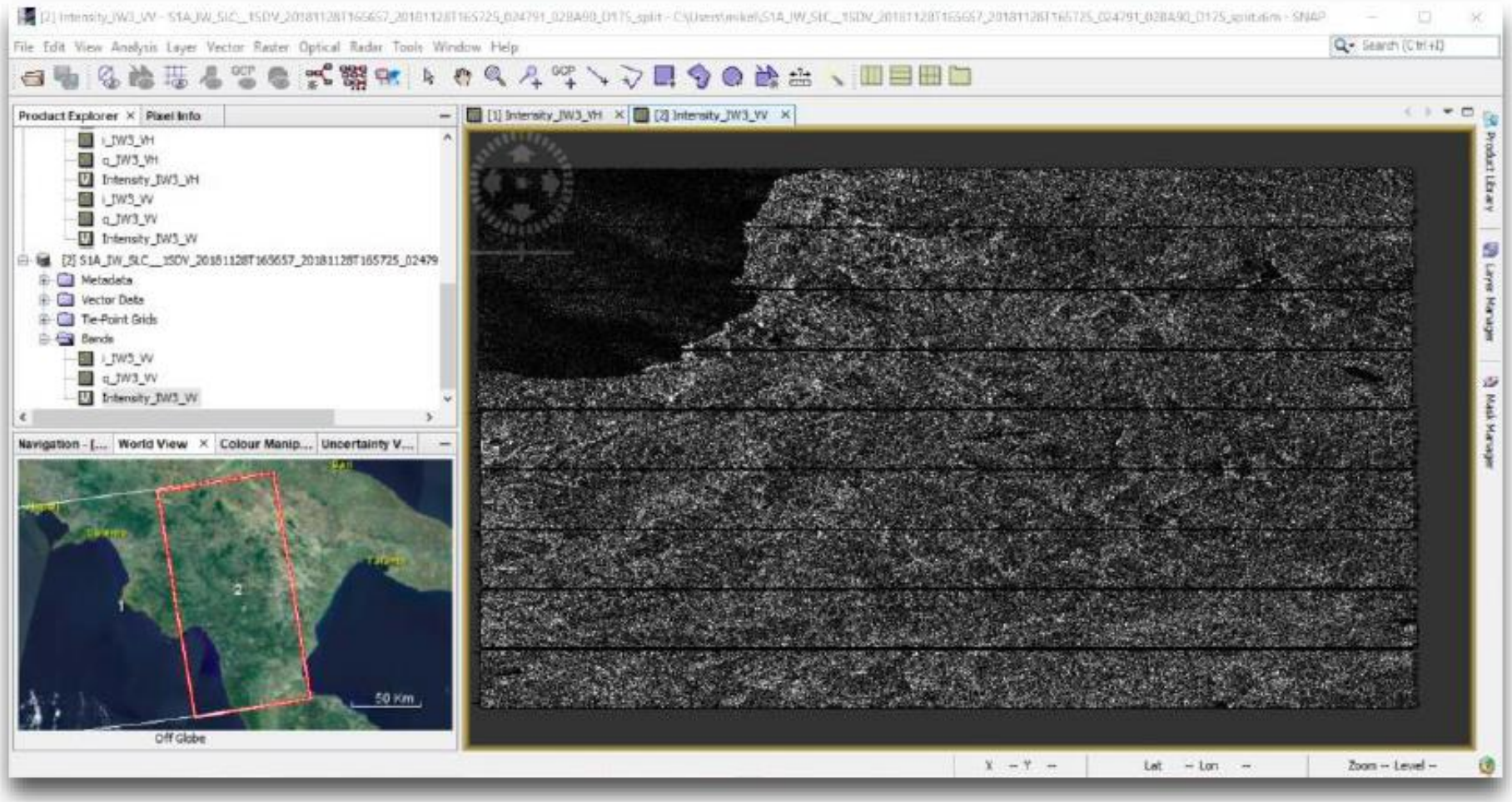
File Edit View Analysis Layer Vector Raster Optical Radar Tools Window Help
Product Explorer
Pixel Info
i_IW3_VH
q_IW3_VH
Intensity_IW3_VH
i_IW3_VV
q_IW3_VV
Intensity_IW3_VV
Metadata
Vector Data
Tie-Point Grids
Bands
Navigation - [...
World View
Colour Manip...
Uncertainty V...
50 Km
Off Globe
[1] Intensity_IW3_VH
[2] Intensity_IW3_VV
Product Library
Layer Manager
Mask Manager
Lat
Lon
Zoom – Level –

Bursting

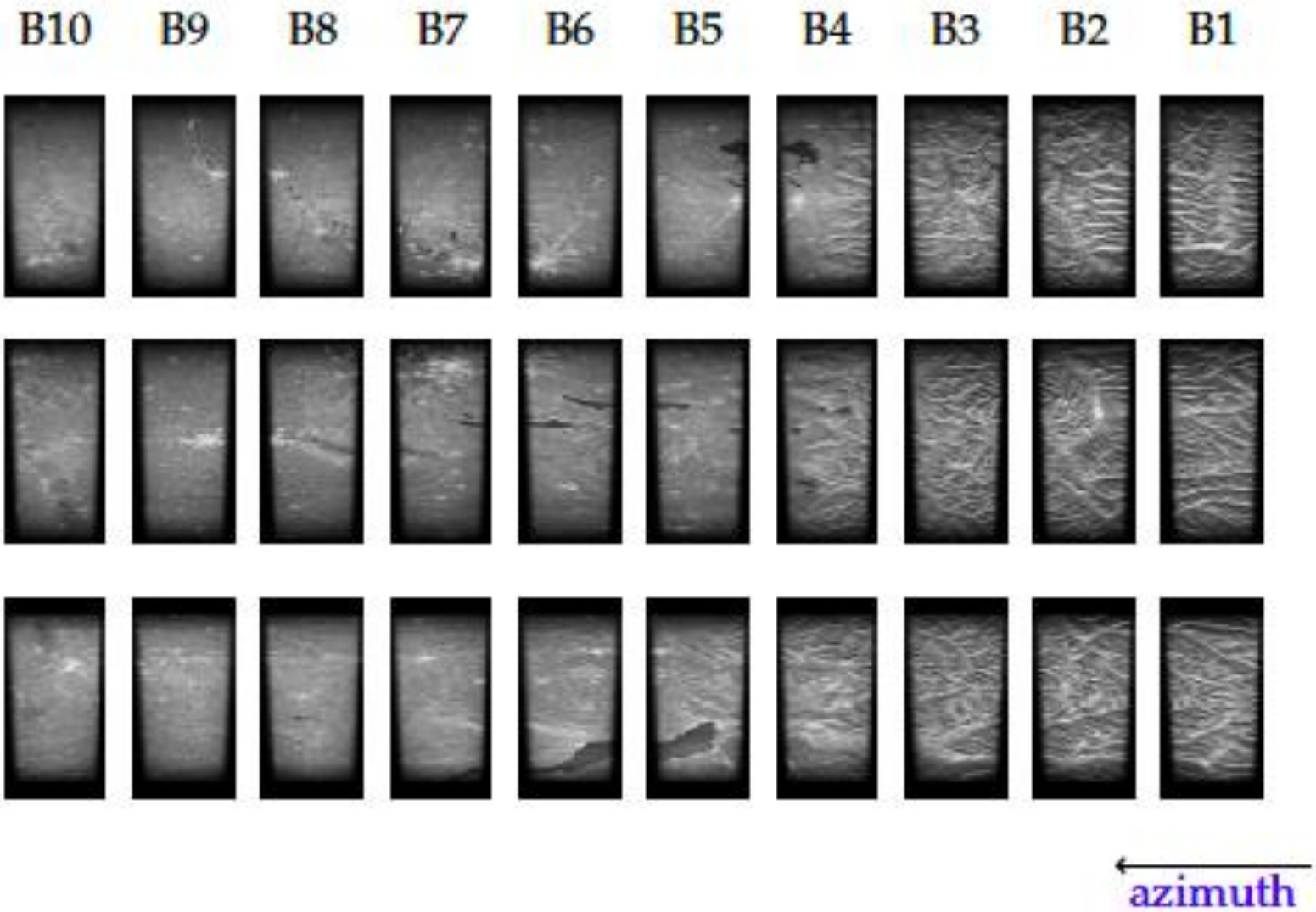

SAR signal characteristics

A SAR resolution cell is very large when compared to the wavelength of the illuminating wave and a large number of scatterers is generally present due to the roughness of the surface and/or the inhomogeneities of the scattering volume. The returned echo is the result of the coherent summation of all the returns due to the single scatterers. For a moving system these contributions change with time and the received signal changes accordingly. This fluctuation in the received signal is referred to as *fading*.

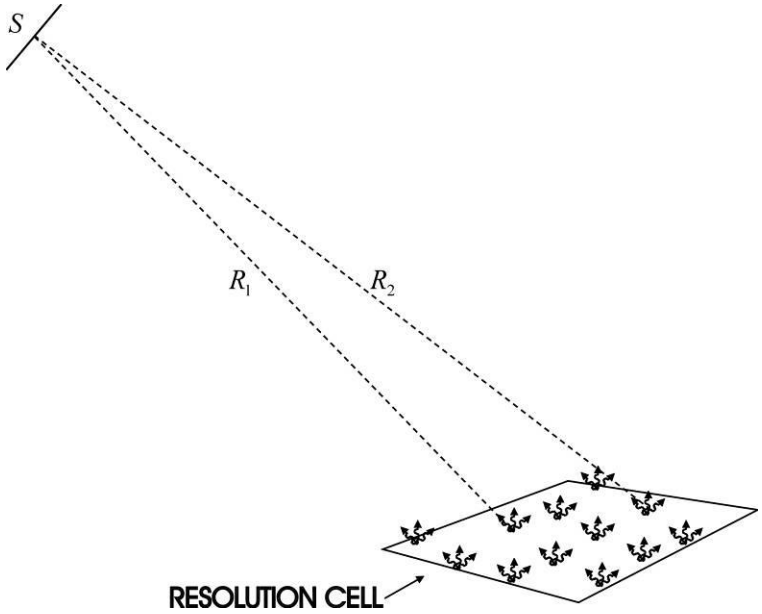

To characterize the SAR image statistical properties we assume that there is no dominant target in the resolution cell and that the number of scatterers *N* is large. In this case, under the further assumptions that the real and imaginary part of the signal are uncorrelated, we have zero mean and standard deviation σ, we conclude that the <u>phase signal is uniformly distributed</u> in $(0,2\pi)$:

and the <u>module signal is Rayleigh distributed</u> in :

$$p(\phi)=\int_0^{\infty} dV\, p(V,\phi)=\frac{1}{2\pi} \qquad (0,\infty)$$

$$p(V)=\int_0^{2\pi} d\phi\, p(V,\phi)=\frac{V}{\sigma^2}\exp\left(-\frac{V^2}{2\sigma^2}\right),\ V\geq 0,$$

with

$$\mathrm{E}[V]=\int_0^{\infty} dV\, p(V)V=\sqrt{\frac{\pi}{2}}\sigma \qquad \textbf{and} \qquad \mathrm{E}\left\{\left[V-\mathrm{E}[V]\right]^2\right\}=\frac{4-\pi}{2}\sigma^2$$

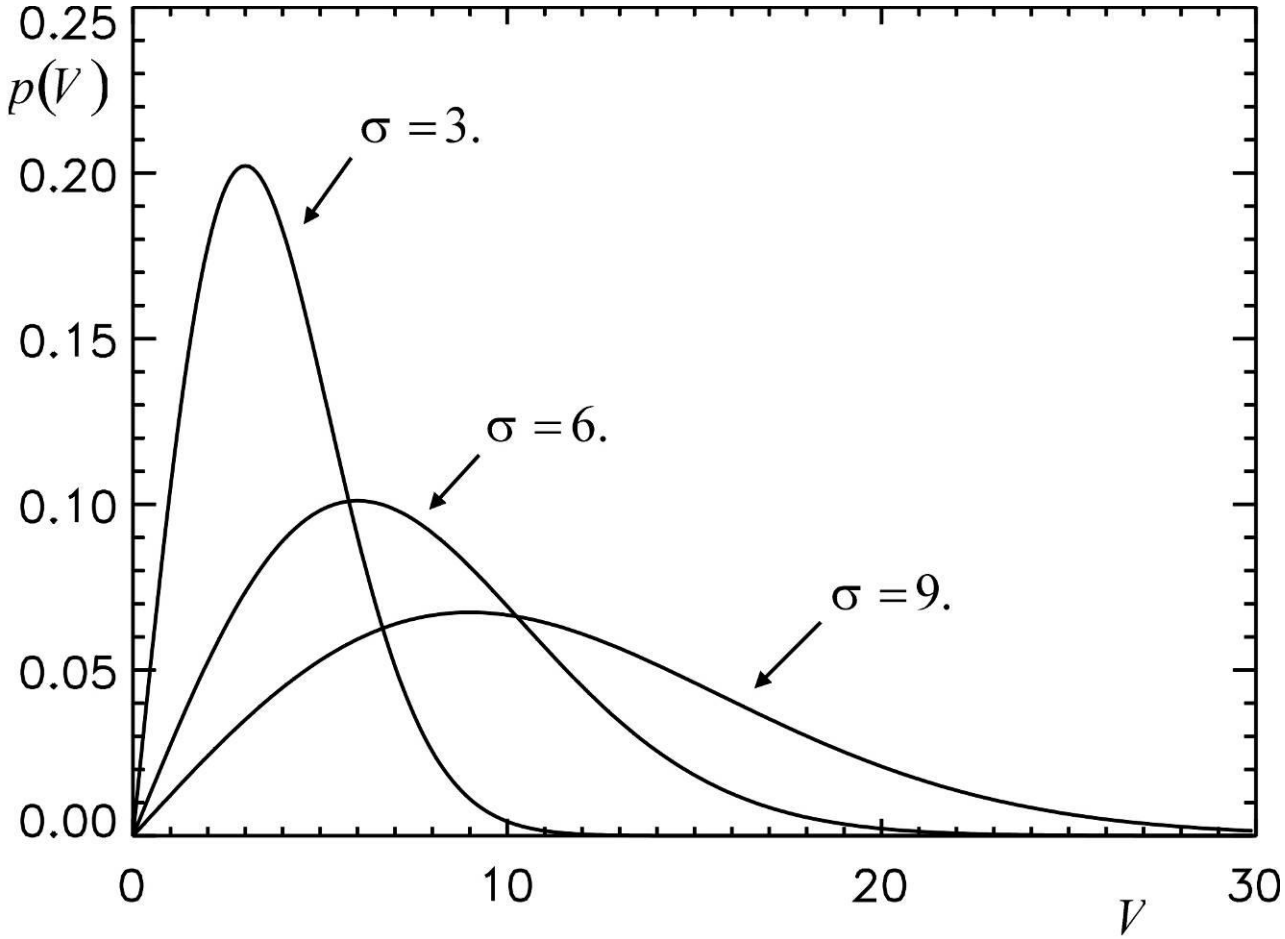

Rayleigh distributions for different σ

Moreover the power signal *W* is exponentially distributed

$$p(W) = \frac{1}{2\sigma^2}\exp\left(-\frac{W}{2\sigma^2}\right)$$

with $\mathrm{E}[W] = 2\sigma^2$ **and** $\mathrm{E}\left\{[W - \mathrm{E}(W)]^2\right\} = [\mathrm{E}(W)]^2 = 4\sigma^4$

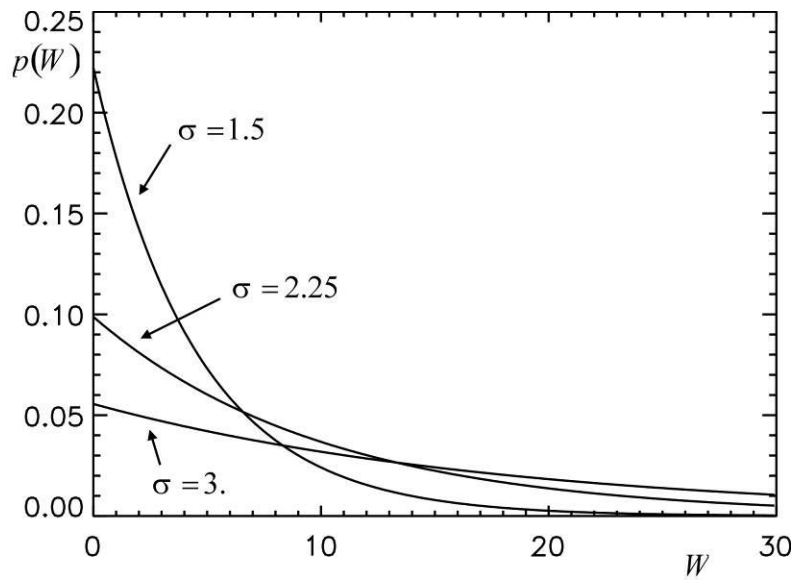

Exponential distributions for different σ

These considerations lead to a popular techniques to reduce the speckle effect, referred to as *multilook*. It consists of first dividing and then separately processing non overlapped portions of the SAR bandwidth. The incoherent average of the so obtained SAR images improves the radiometric resolution; the availability of multi-acquisition images would allow to obtain similar results but with no loss of resolution !

multilook →

Speckle Noise Filtering

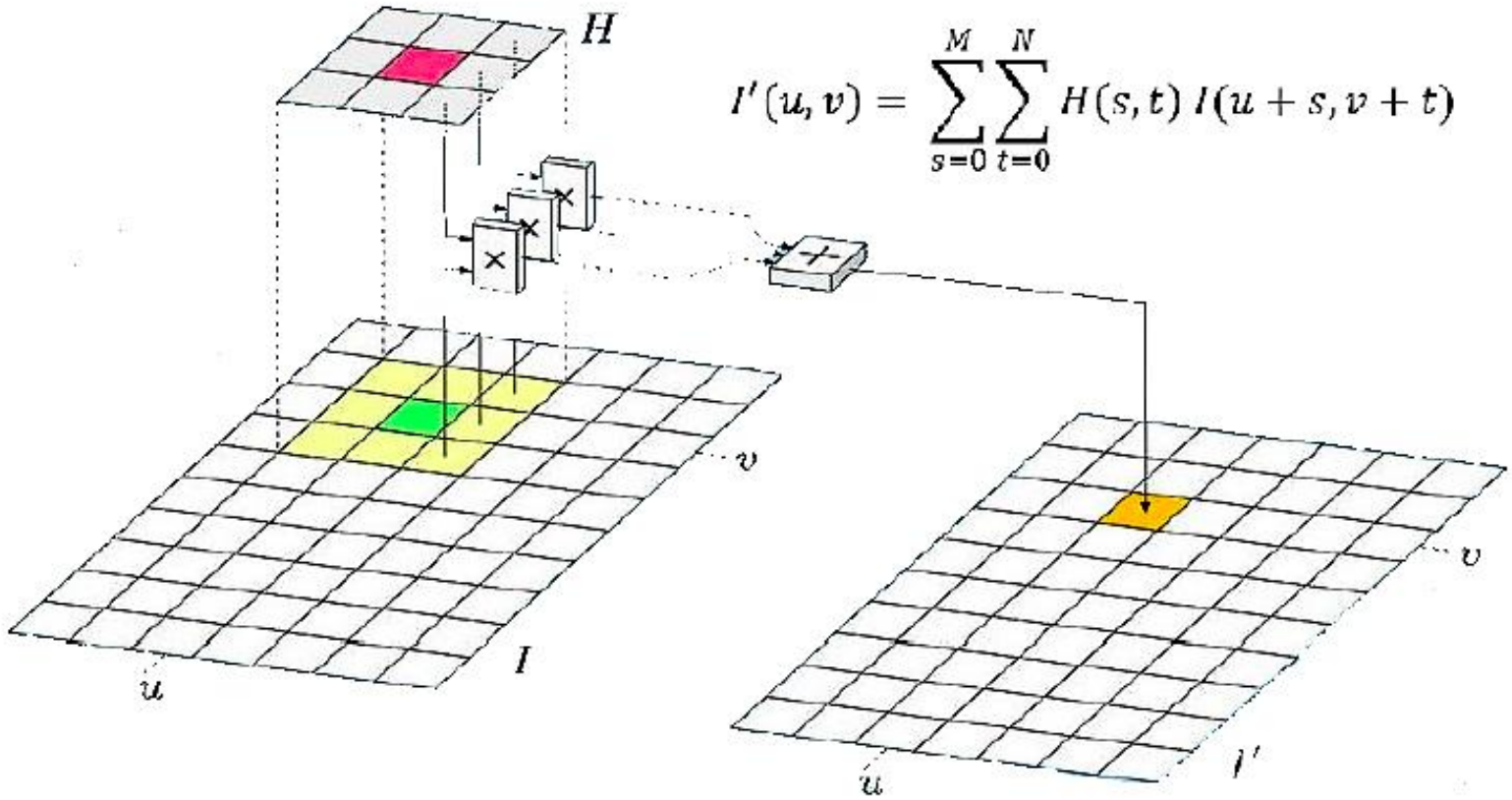

$$I'(u,v) = \sum_{s=0}^{M} \sum_{t=0}^{N} H(s,t)\, I(u+s, v+t)$$

Speckle Noise Filtering

A. Lee Filter

The Lee filters [8], [9] compute a linear combination of the center pixel intensity in a filter window with an average intensity of the window for removing speckle noise. This filter based on the minimum mean square error (MMSE), and for producing speckle free image governed by the following relationship:

$$\hat{R}(t) = \bar{I}(t) + W(t)(I(t) - \bar{I}(t)) \tag{2}$$

where $\hat{R}(t)$ is image value after being filtered and it's also the estimate value of $R(t)$, $\bar{I}(t)$ is the mean value of $I(t)$, and the weighting function $W(t)$ is given by

$$W(t) = 1 - \frac{C_v}{C_I} \tag{3}$$

where C_v is the variance coefficient of noise-affected image with standard deviation, and C_I is the variance coefficient of noise-free of local image with standard deviation.

Speckle Noise Filtering

FROST

$$W = \exp\left(-K \frac{|t - t_0|}{ENL}\right)$$

MEDIAN

123	125	126	130	140
122	124	126	127	135
118	120	150	125	134
119	115	119	123	133
111	116	110	120	130

Neighbourhood values:

115, 119, 120, 123, 124,
125, 126, 127, 150

Median value: 124

Speckle Noise Filtering

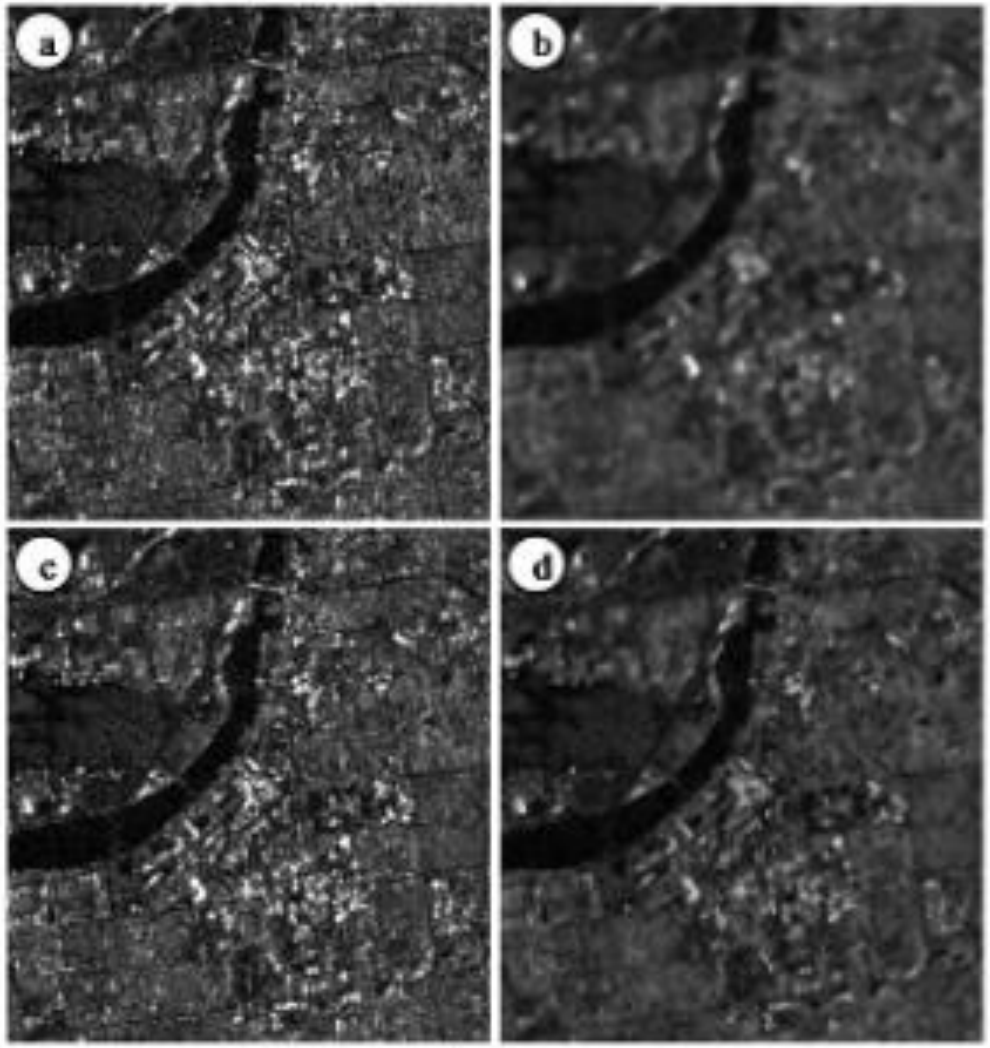

(a) Original

(b) Median Filter

(c) Frost Filter

(d) Lee Filter

$$SNR = 10\, log_{10} \frac{\sum_{i=1}^{K} S_i^2}{\sum_{i=1}^{K} \left(\hat{S}_i - S_i\right)^2}$$

SAR Temporal Multi-Look

Temporal Multi-Look

To increase ISNR, without reducing spatial resolution, we may incoherently average homologous pixels belonging to SAR images acquired at <u>different epochs</u>, properly co-registered to a reference master image.

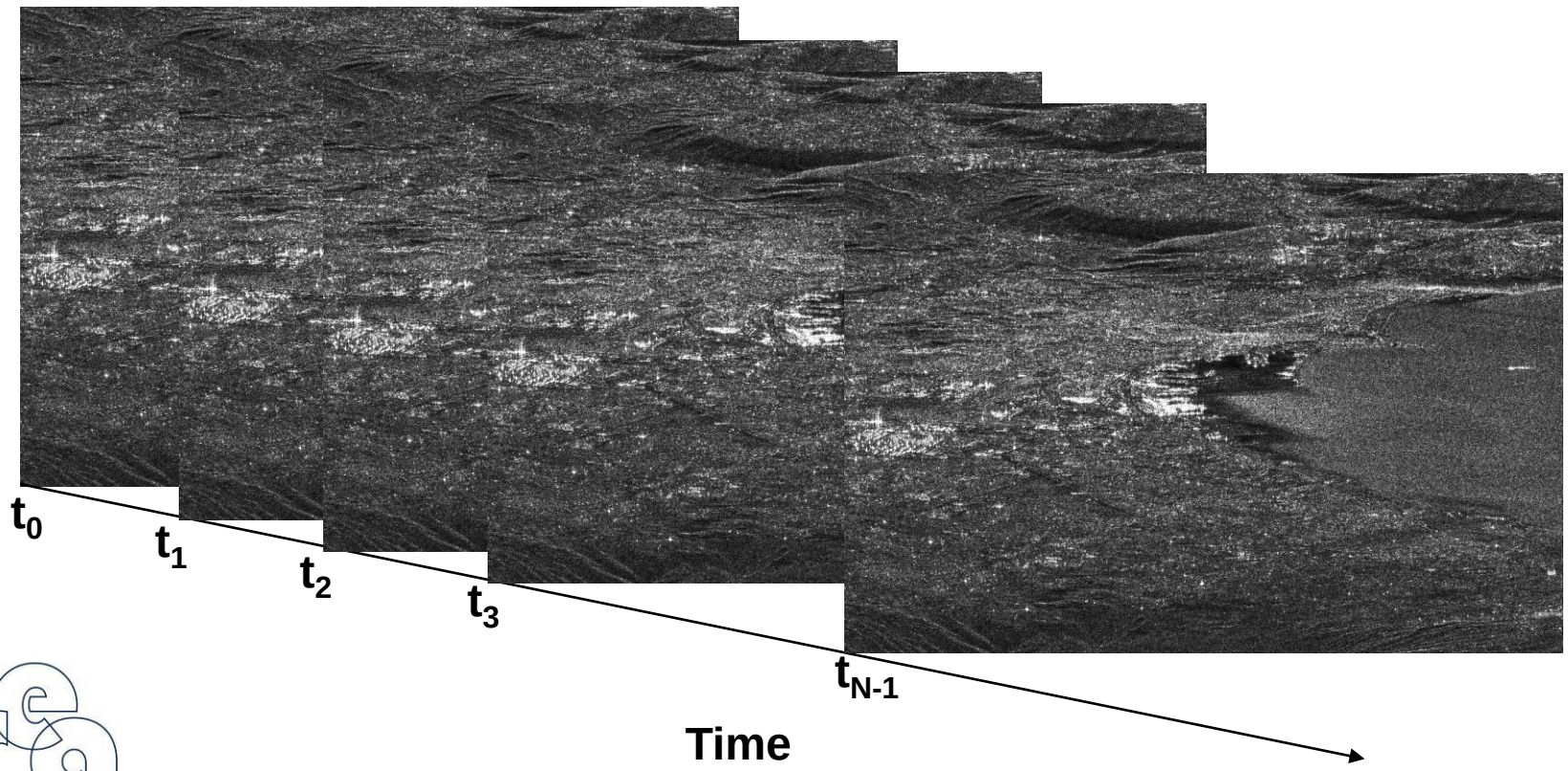

Multilook SAR Image

RADAR CROSS SECTION

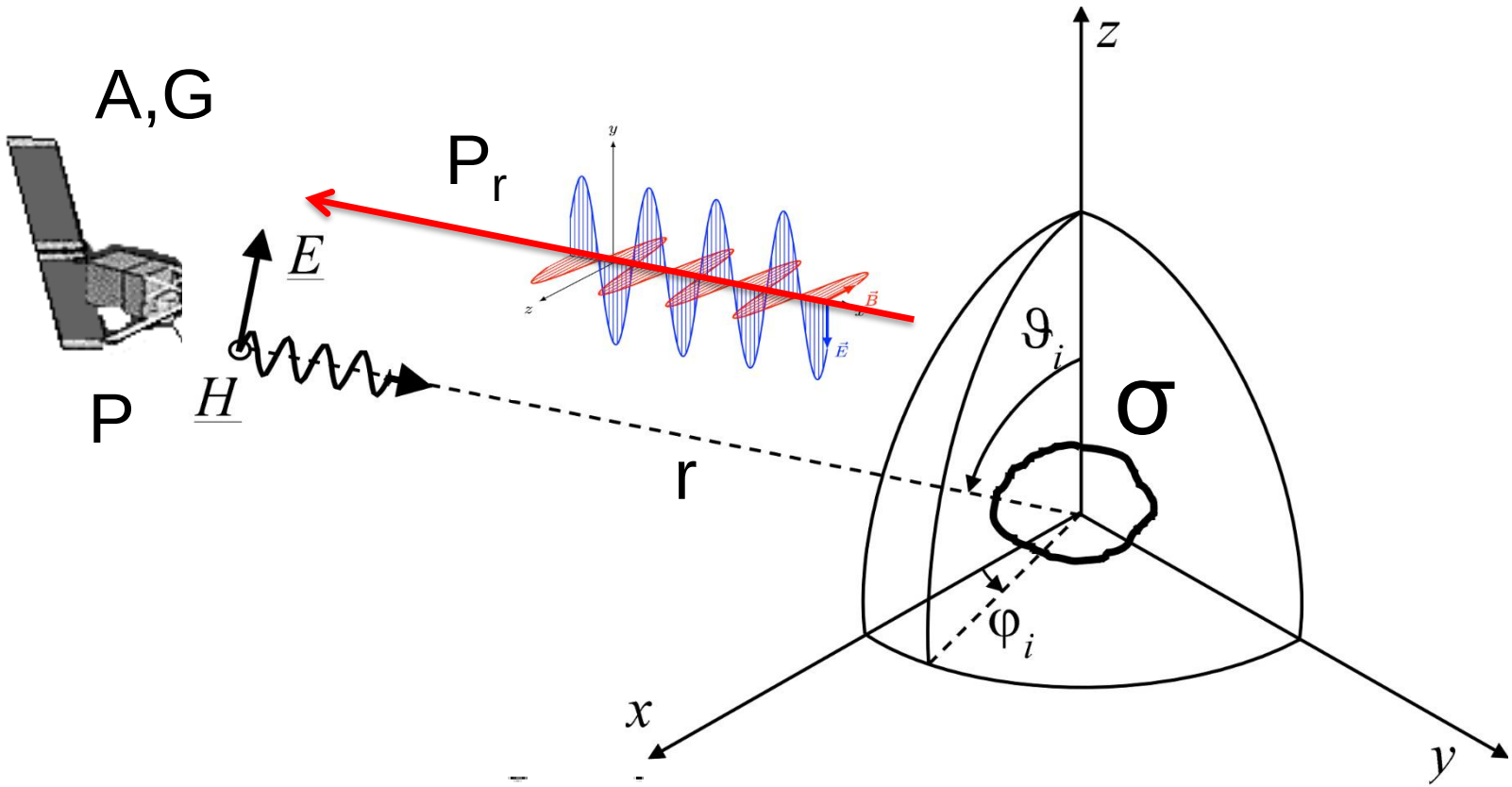

$$P_r = \frac{PGA\sigma}{(4\pi)^2 r^4} = \frac{PG^2\lambda^2\sigma}{(4\pi)^3 r^4} = \frac{PA^2\sigma}{4\pi\lambda^2 r^4}$$

Sigma Nought

$$\sigma^0 = \frac{\sigma}{\Delta x \Delta r} = |\gamma|^2$$

Rules-of–Thumb in Backscatter Radar Images

Backscatter range	***Possible explanation***
Very High Backscatter (above –5dB)	• Terrain slopes towards radar • Radar looking almost straight down • Very rough surface • Flooded forest • Man-made objects
High Backscatter (-10 to 0dB)	• Rough surface • Dense vegetation, e.g. forest
Moderate Backscatter (-20 to 10dB)	• Moderately rough surface • Medium level of vegetation, e.g. shrubs, agricultural crops
Low Backscatter (below -20dB)	• Terrain slopes away from radar • Smooth surface, e.g. water, road surface • Very dry material, e.g. sand in a arid desert

RADAR IMAGES ARE MAPS OF THE AVERAGE RADAR CROSS SECTIONS AFTER RADIOMETRIC CALIBRATION

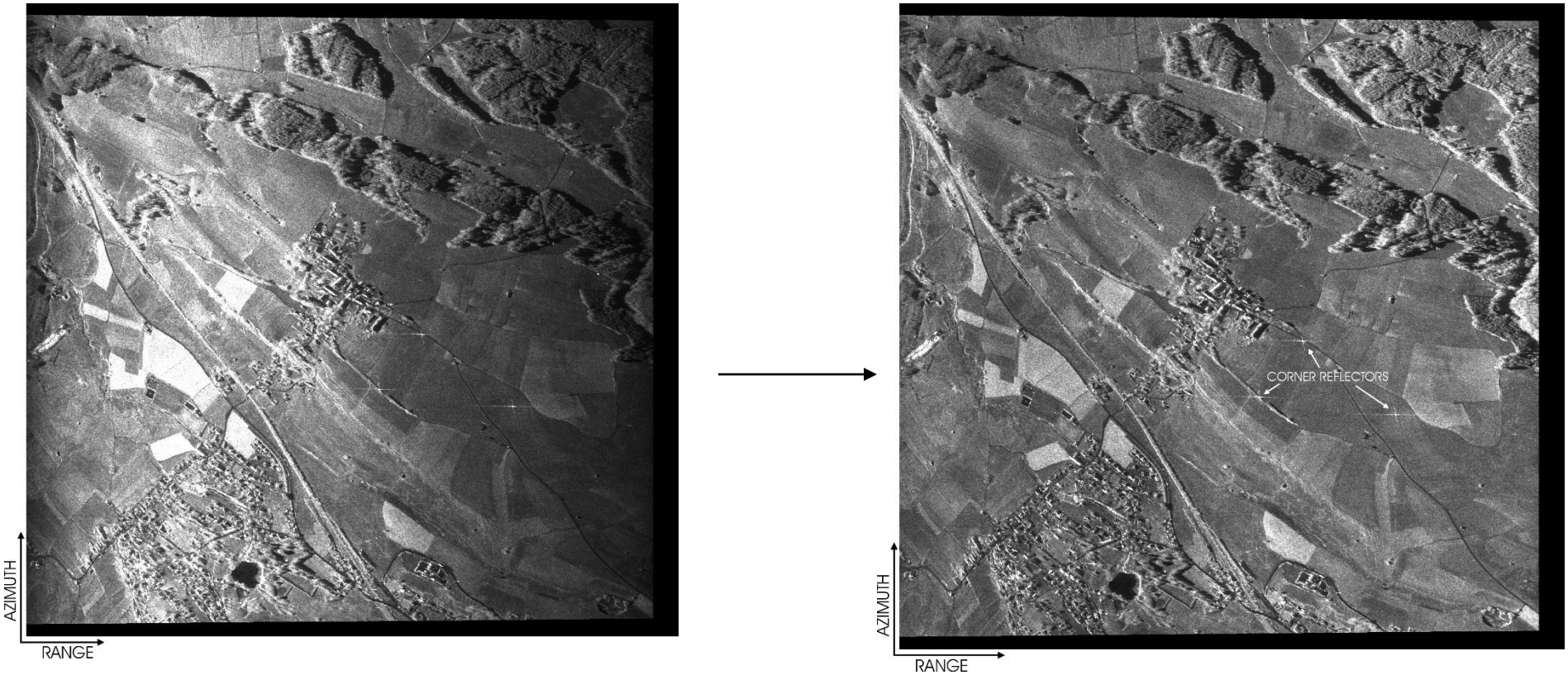

Uncalibrated (left) and calibrated (right) SAR image including three corner reflectors; note The effect of the uncompensated antenna gain factor (Courtesy of AeroSensing RadarSysteme).

Radiometric Calibration of SAR Images
Correction of Topography

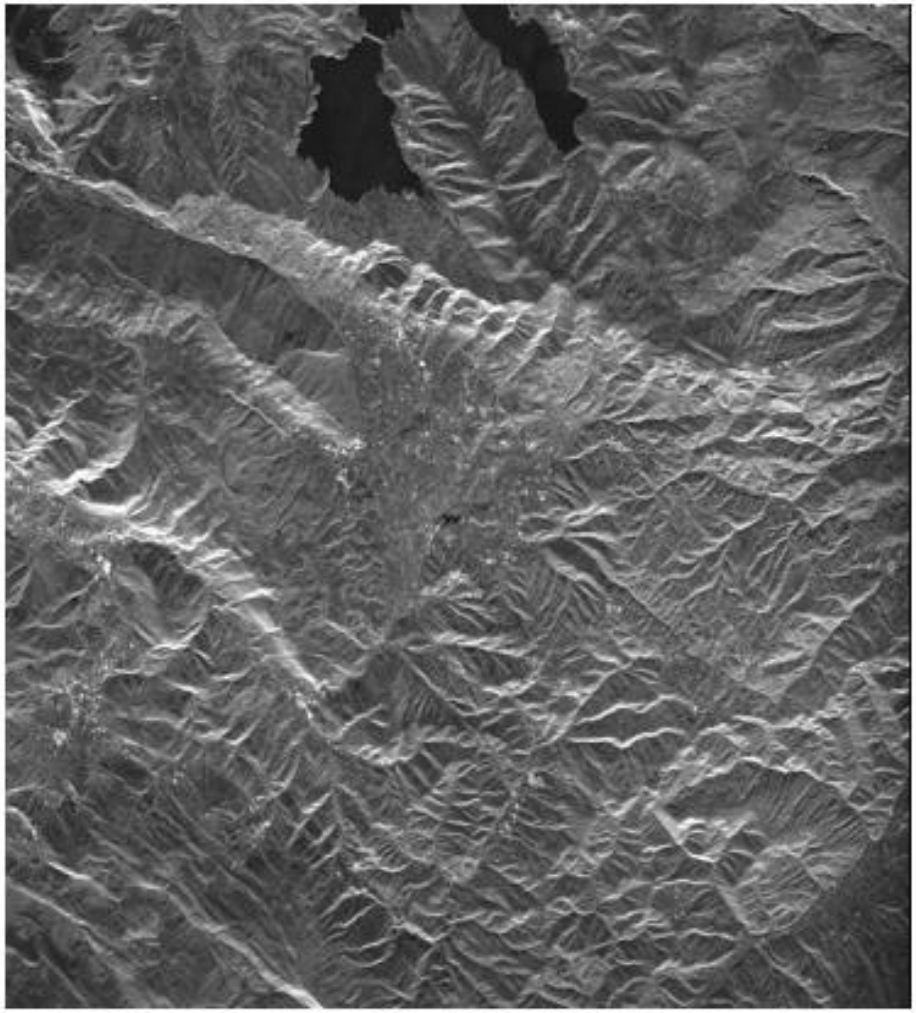

Fig.1. SLC COSMO-Skymed SAR amplitude image.

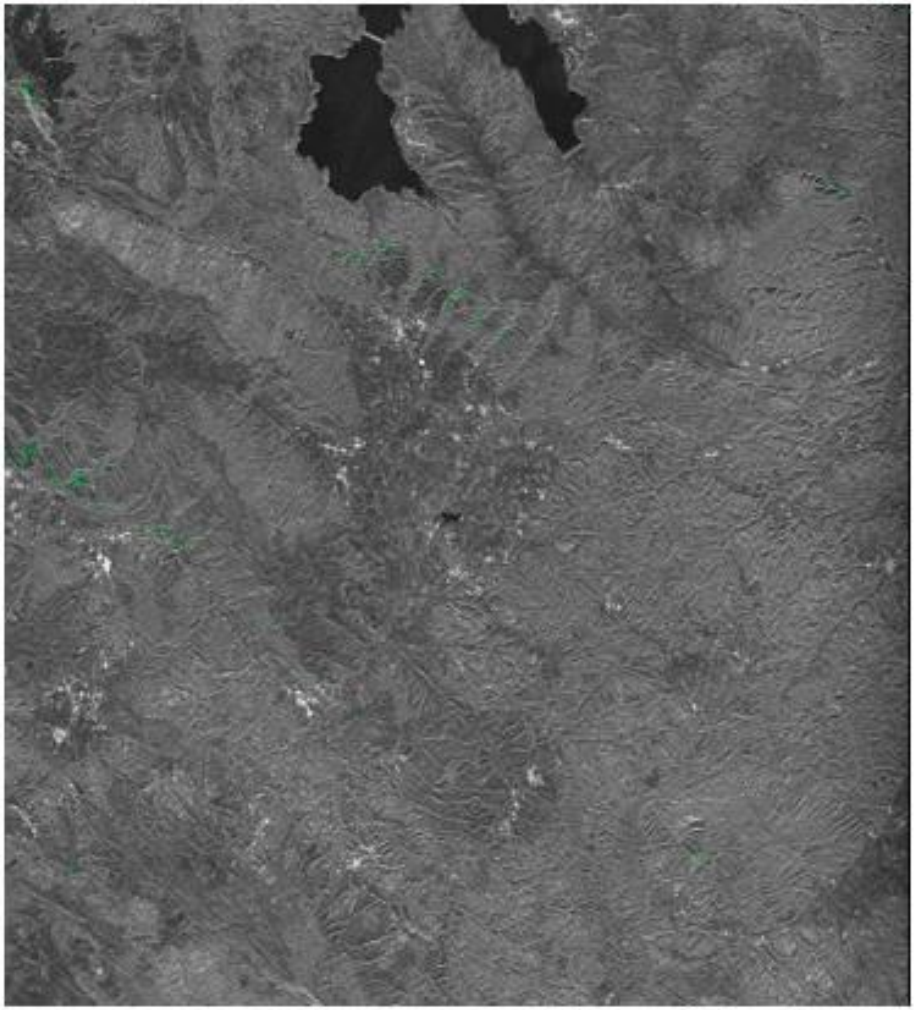

Fig. 2. Calibrated COSMO-Skymed SAR image obtained by applying the GICAL processing scheme. A layover mask (in green) is also superimposed.

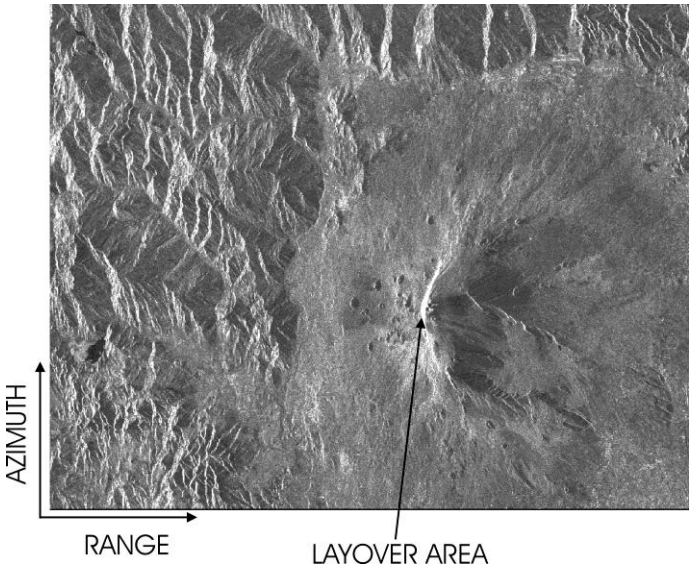

← **SAR geometry**

Cartographic reference (UTM projection) →

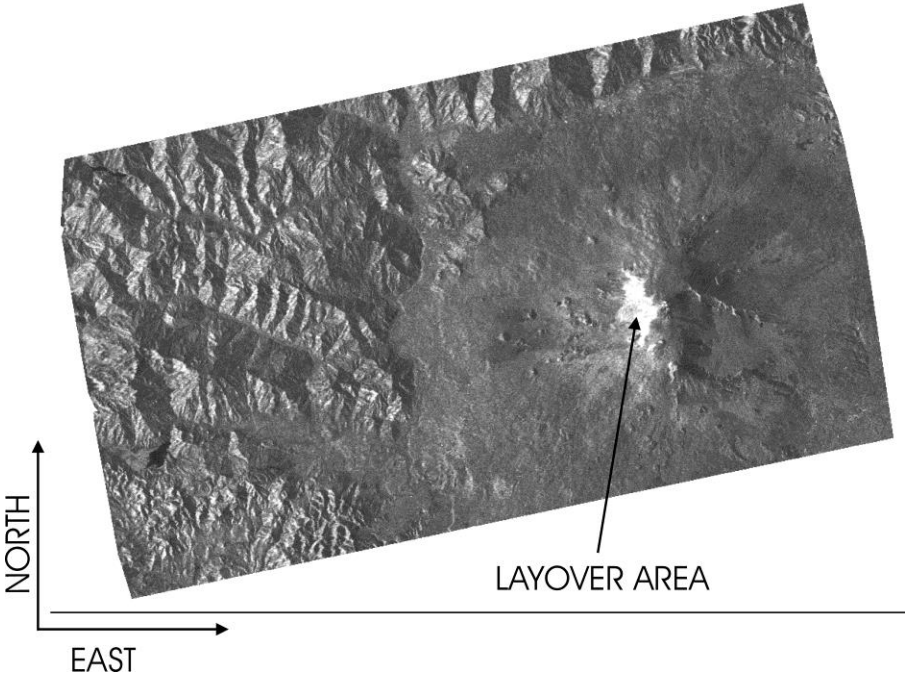

Overview

Fire is a GLOBAL ISSUE:
On Earth, something is always burning!

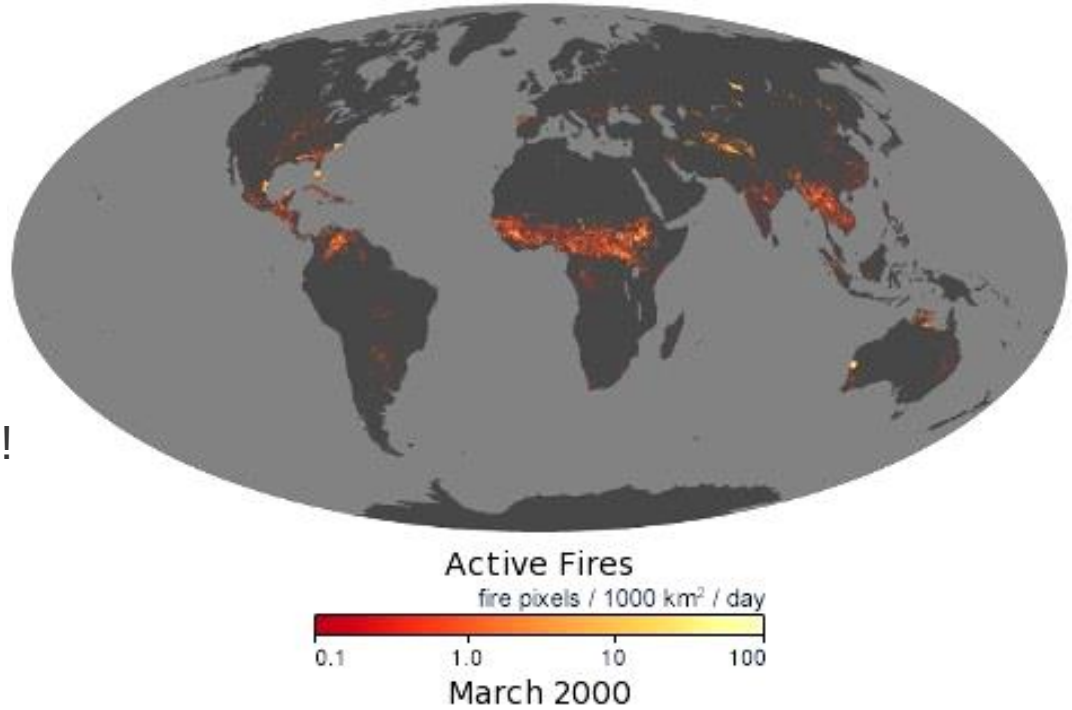

- Fire is one of the most dangerous hazards for human life and good
- Severe damage to natural ecosystems and agriculture
- Major source of atmospheric trace gases and aerosol particles that affect the composition of the atmosphere and the global climate

Optical and Microwave Fire Detection

- Detection, mapping and monitoring burned areas is relevant for the prevention/mitigation of the fire associated risk
- Satellite data are a valuable source for mapping/monitoring areas affected by fires

- Research framework developed for OPTICAL DATA

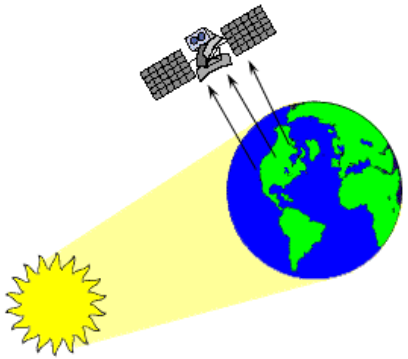

Optical and Microwave Fire Detection

- Detection, mapping and monitoring burned areas is relevant for the prevention/mitigation of the fire associated risk
- Satellite data are a valuable source for detecting/mapping/monitoring areas affected by fires
- Research framework developed for OPTICAL DATA

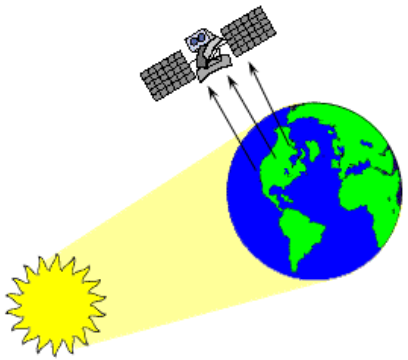

- low frequency acquisition (clouds)
- high variability of spectral properties of burned surfaces as a function of: pre-fire vegetation characteristics and conditions, fire intensity, fire type, post-fire processes, vegetation regrowth
- spectral confusion with low albedo surface targets (water, cloud and topographic shadows, sparse vegetation, etc)

Optical and Microwave Fire Detection

- Detection, mapping and monitoring burned areas is relevant for the prevention/mitigation of the fire associated risk
- Satellite data are a valuable source for detecting/mapping/monitoring areas affected by fires

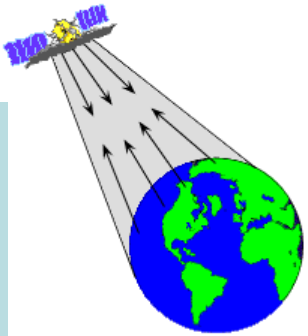

Integration optical and SAR data has been not fully addressed:

i. Few (or none) operative satellite SAR mission are available (were available before Sentinels);
ii. Few large area studies on the effect of fire affected areas on backscatter (mainly in forested areas);
iii. Poor performance for mapping fire in non forested vegetation;

Burned Areas Mapping:Experiments in Portugal

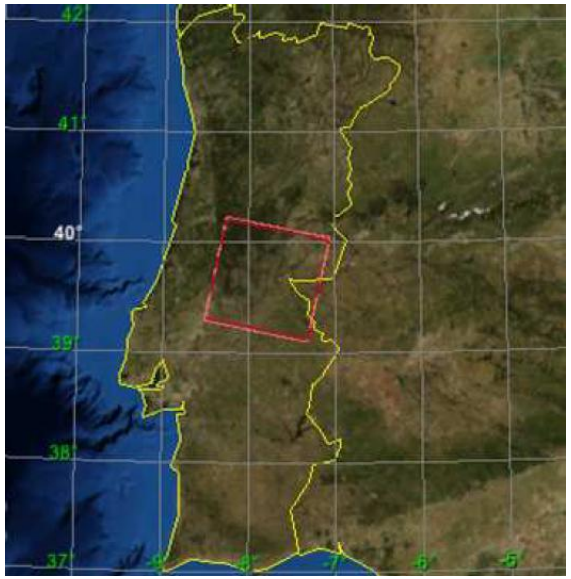

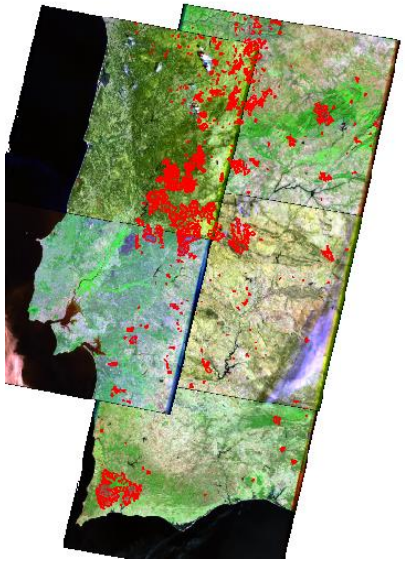

Available SAR dataset	
Sensor	Envisat
Orbit	Descendent
Track	180
Number of images	20
Time interval	11/05/2003 – 20/12/2009

Burned Areas Mapping:Experiments in Portugal

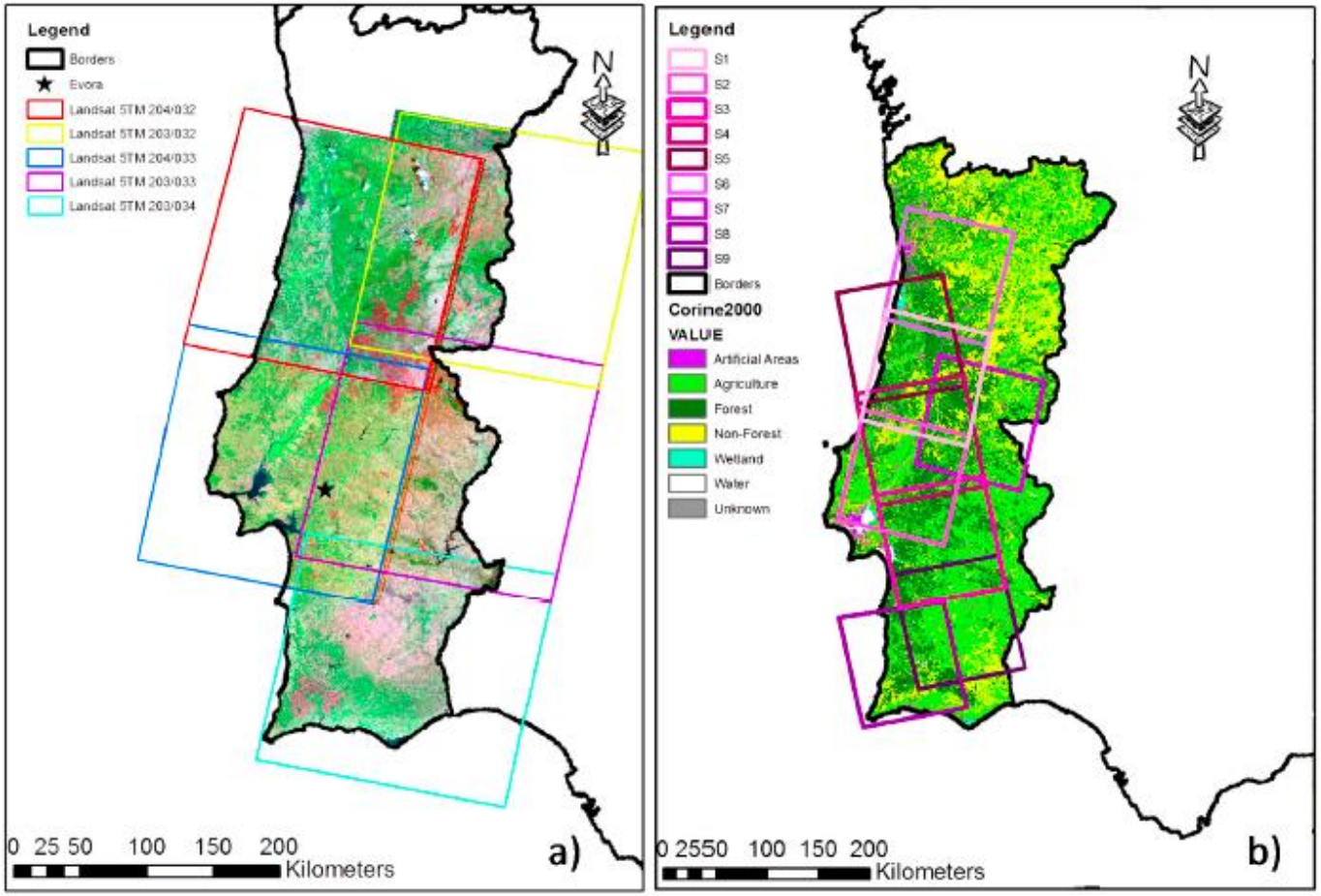

Figure 1. Optical and SAR datasets acquired during the year 2003 and used for this study: (**a**) Landsat-5 TM images shown as false color composite mosaic (R-G-B: 5-4-3); (**b**) ENVISAT ASAR data frames overlaid on the Corine Land Cover (CLC2006) map. Lists of optical and SAR scenes are given in Tables 1 and 2.

Burned Areas Mapping:Experiments in Portugal

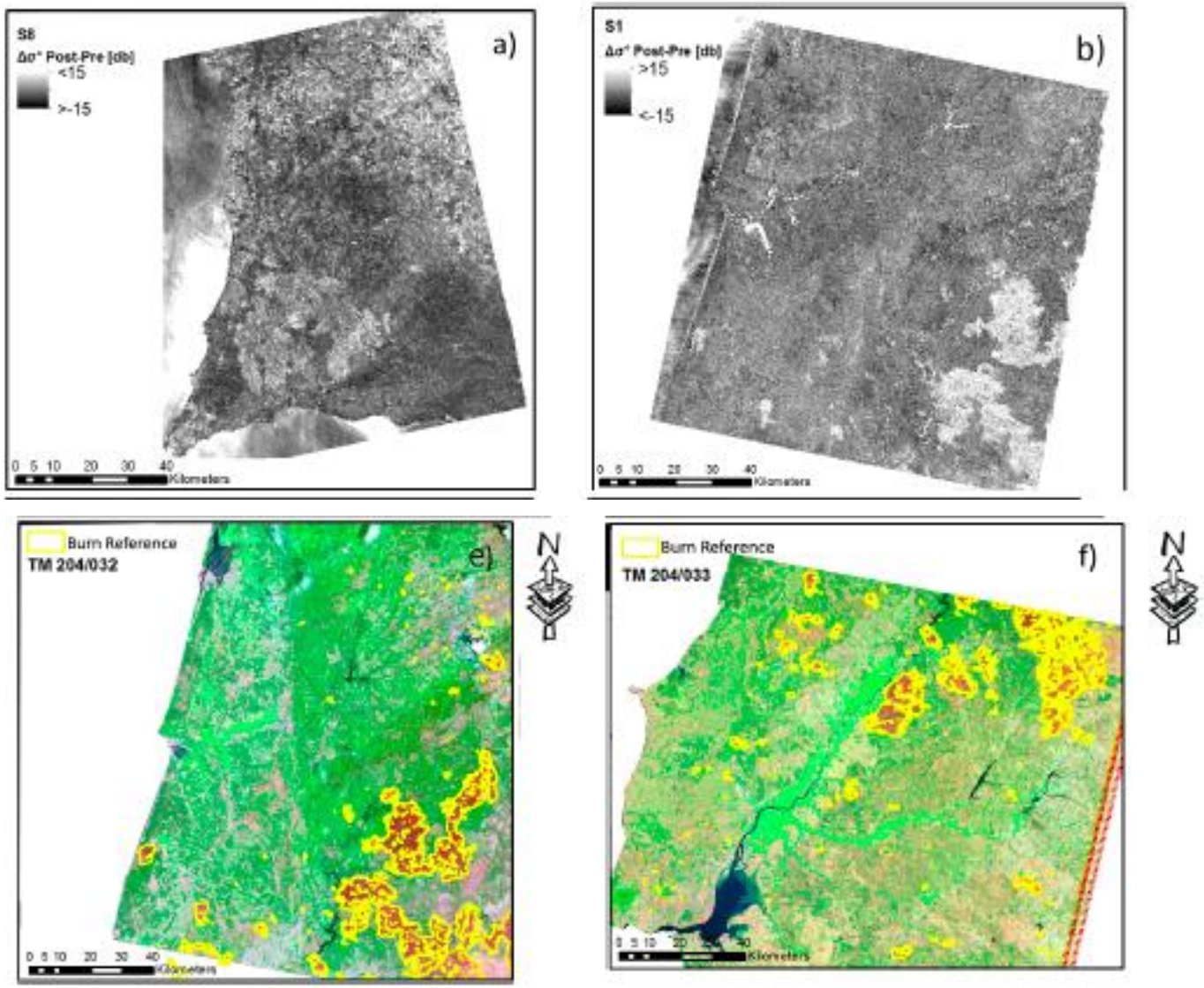

Stroppiana et al. 2015, “Integration of Optical and SAR Data for Burned Area Mapping in Mediterranean Regions,“Remote Sens. 2015, 7, 1320-1345; doi:10.3390/rs7020

Burned Areas Mapping:Experiments in Portugal

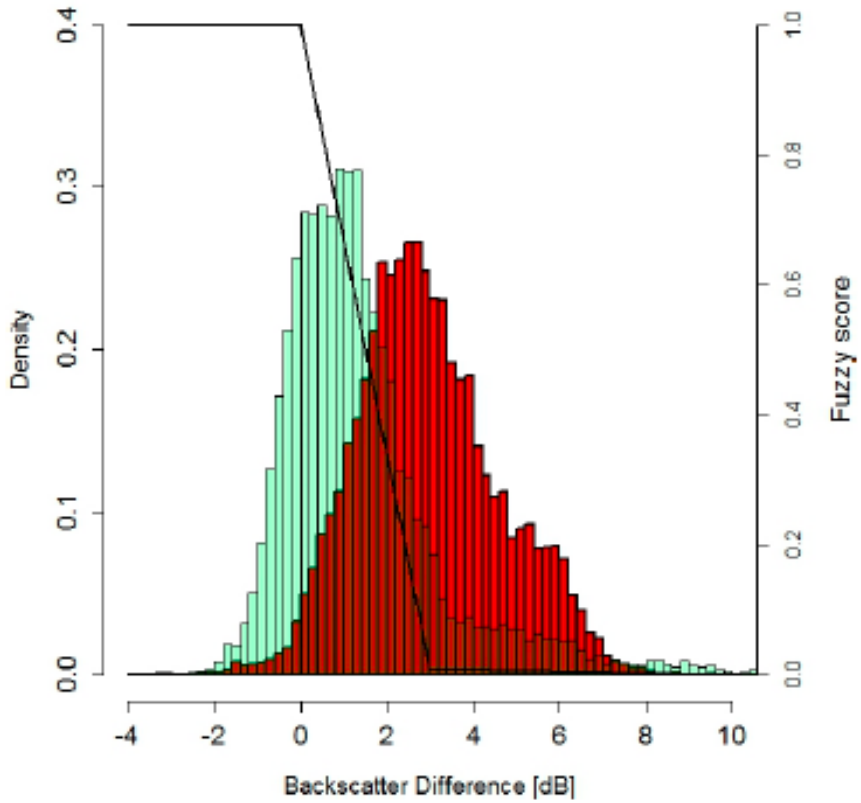

Figure 5. The histograms of $\Delta\sigma°$ values over burned (red) and unburned (green) surfaces (unburned vegetation, soil/sparse vegetation and urban all together) shown as probability density. On the secondary y-axis the score given by the membership function of fuzzy sets ($\mu_{\Delta\sigma°}$ for the negative evidence as defined by Equation (2).

Burned Areas Mapping:Experiments in Portugal

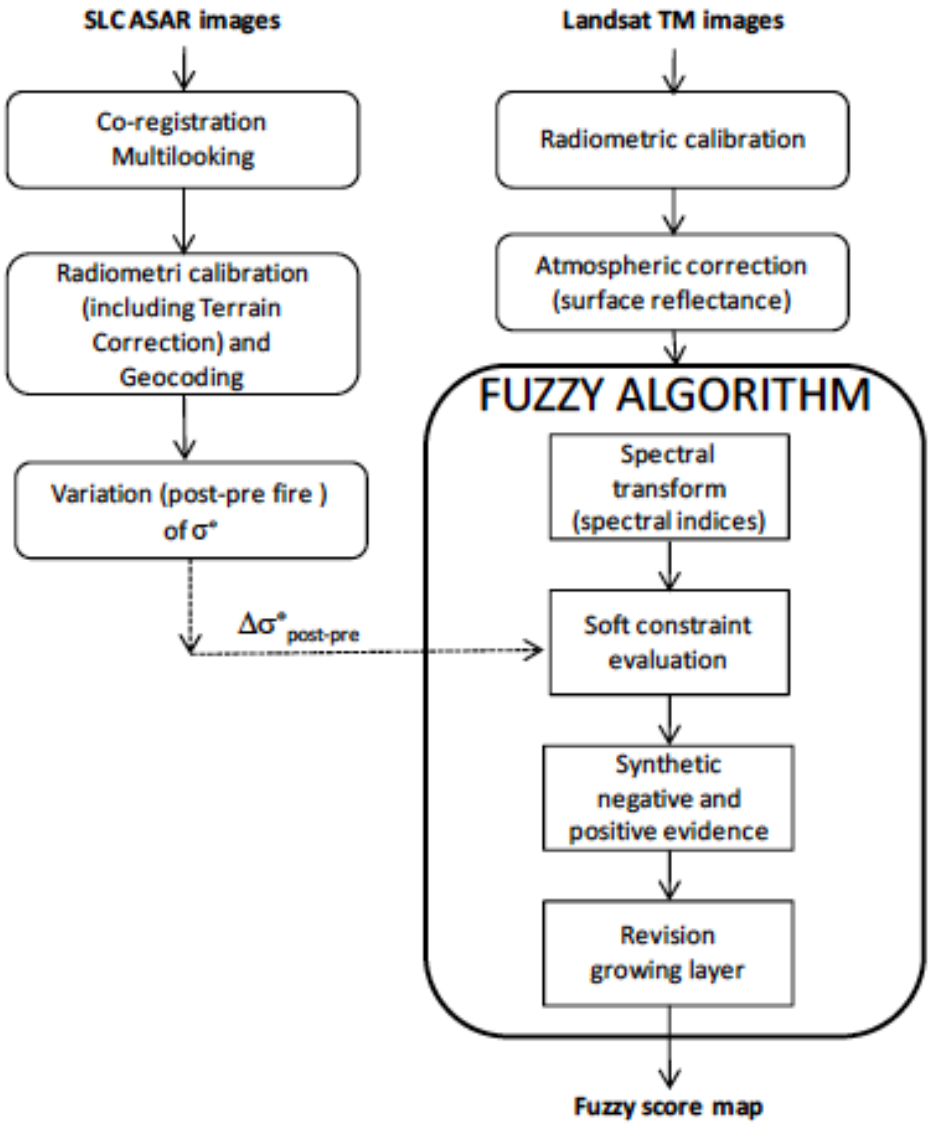

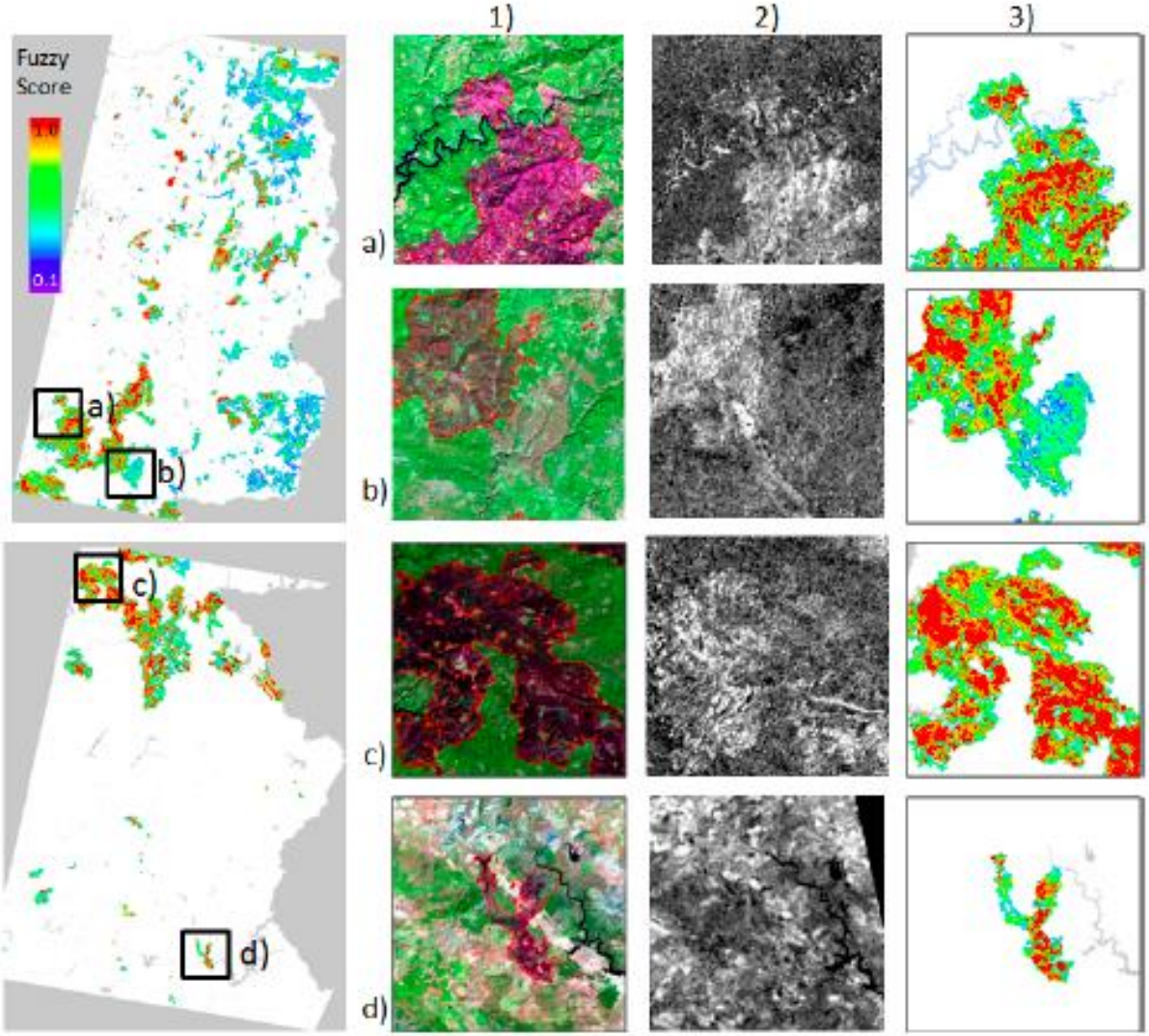

Figure 7. (a–d) Examples of the optical + SAR fuzzy score maps (column 3) over zoom areas of about 22 km × 22 km from TM frames 203/032 (rows a, b) and 203/033 (bottom) (rows c, d) compared to the Landsat TM (R-G-B 5-4-3) (column 1) and the $\Delta\sigma^{\circ}$ images (column 2). The red polygons are the reference fire perimeters.

Using Polarimetric SAR Data

remote sensing

MDPI

Article

A Simple Normalized Difference Approach to Burnt Area Mapping Using Multi-Polarisation C-Band SAR

Jeanine Engelbrecht [1,2,*], Andre Theron [1,2], Lufuno Vhengani [1] and Jaco Kemp [2]

1 CSIR Meraka Institute, Pretoria 0001, South Africa; atheron1@csir.co.za (A.T.); LVhengani@csir.co.za (L.V.)

2 Department of Geography & Environmental Studies, Stellenbosch University, Stellenbosch 7600, South Africa; jkemp@sun.ac.za

* Correspondence: jengelbrecht@csir.co.za; Tel.: +27-021-888-2447

Academic Editors: Quazi K. Hassan, George P. Petropoulos, Ioannis Gitas and Prasad S. Thenkabail

Received: 12 June 2017; Accepted: 19 July 2017; Published: 31 July 2017

Using Polarimetric SAR Data

$$\mathrm{ND}\alpha\mathrm{I} = \frac{\alpha_{\text{pre-burn}} - \alpha_{\text{post-burn}}}{\alpha_{\text{pre-burn}} + \alpha_{\text{post-burn}}}$$

H-A-α Clode Pottier Decomposition

Cloude, S.R.; Pottier, E. An entropy based classification scheme for land applications ofpolarimetric SAR. IEEE Trans. Geosci. Remote Sens. 1997, 35, 68–78

Using Polarimetric SAR Data

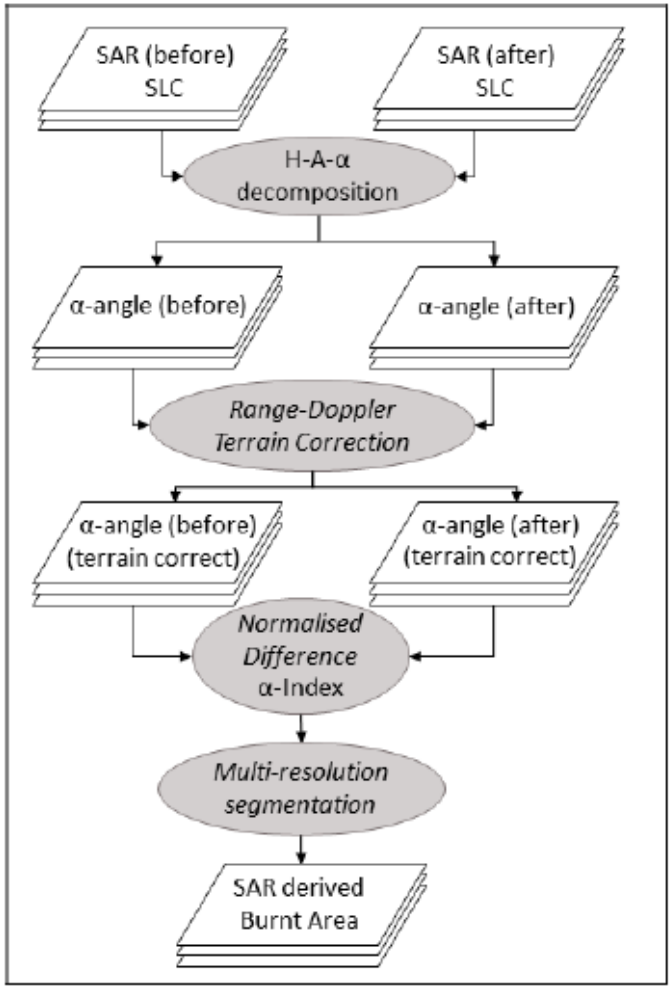

Figure 4. The synthetic aperture radar (SAR) data processing workflow for burnt area mapping (SLC = Single Look Complex).

Using Polarimetric SAR Data

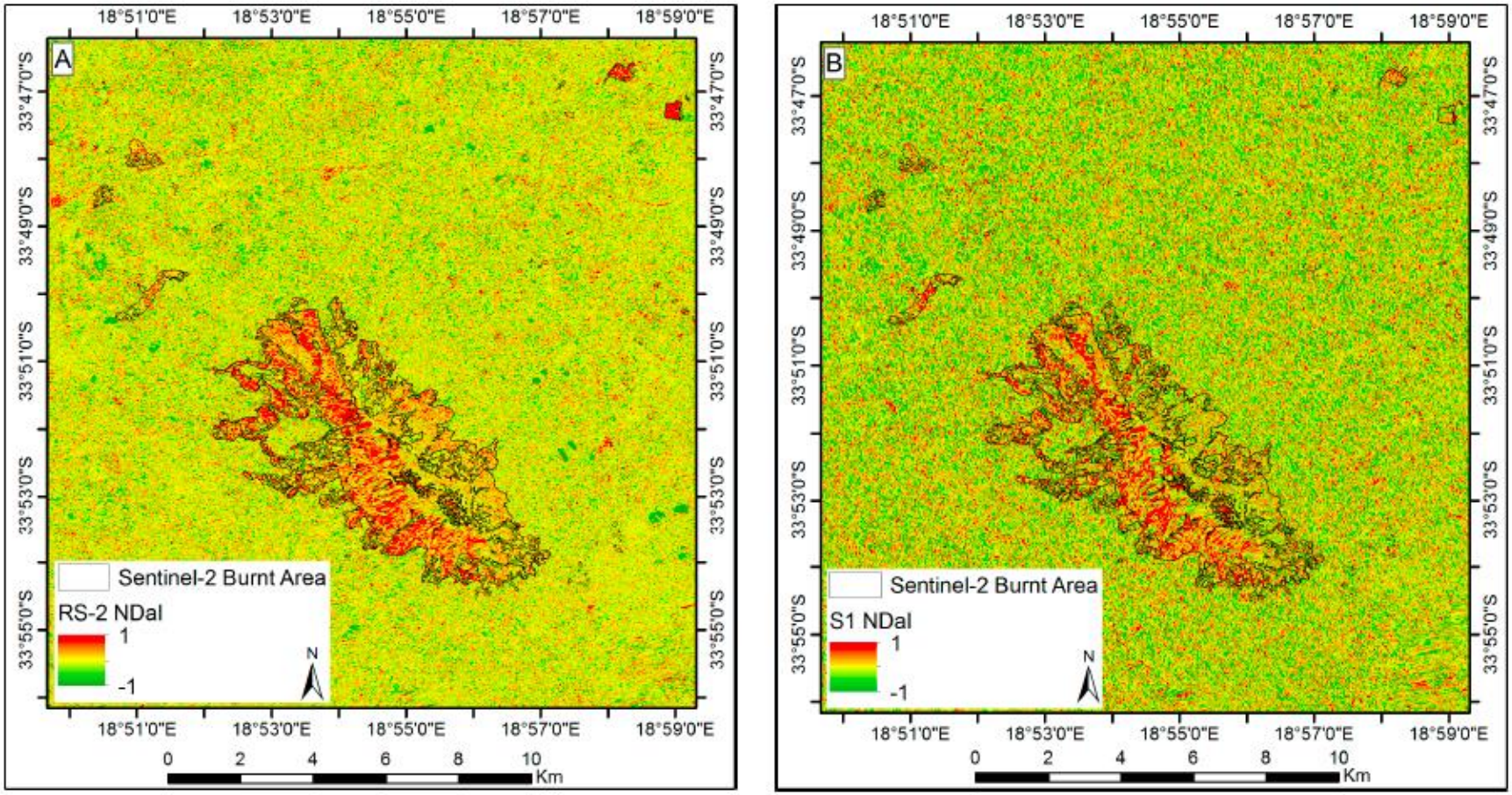

Figure 5. The results of calculating NDαI for Radarsat-2 (RS-2) (A) and Sentinel-1A (S1) (B) data. The extent of the burn scar extracted from Sentinel-2A (black outlines) are also shown for comparison.

Burned Areas Mapping: Experiments with S-1

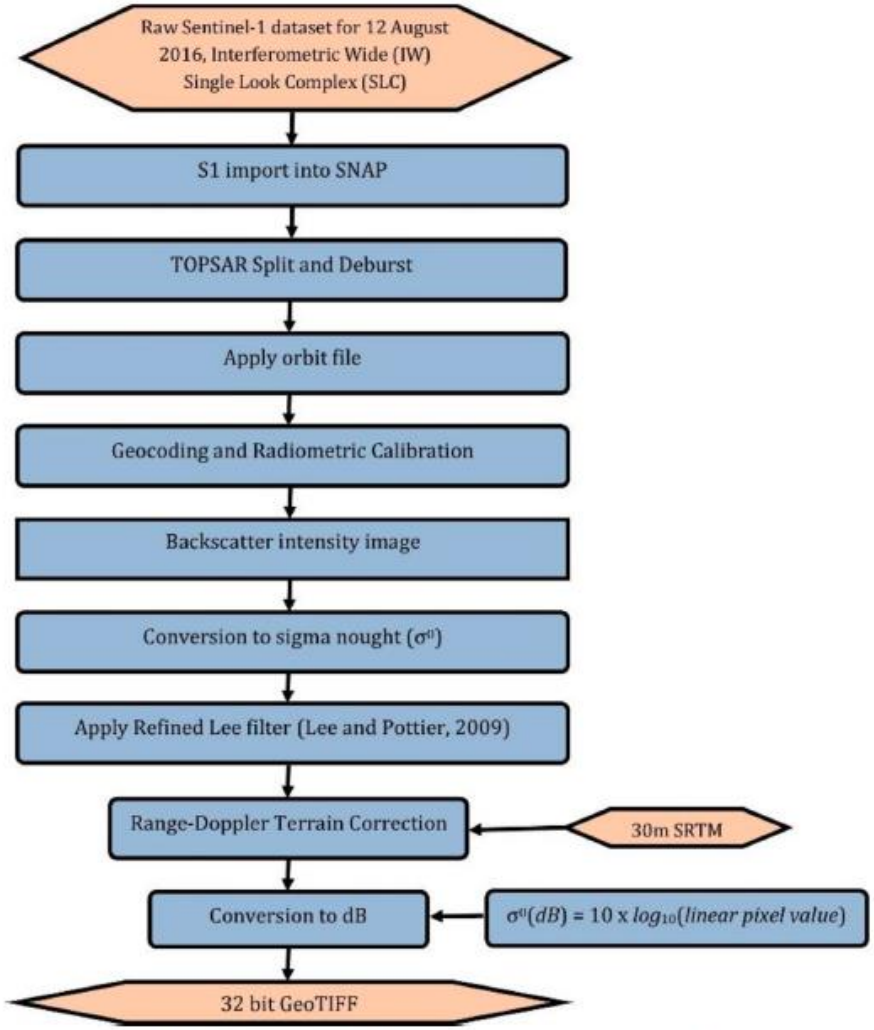

Fig. 2. Methodology work flow for the pre-processing of Sentinel 1.

Colson et al. 2018, "Exploring the Potential of Sentinels-1 & 2 of the Copernicus Mission in Support of Rapid and Cost-effective Wildfire Assessment," Int J Appl Earth Obs Geoinformation 73 (2018) 262–276

Effect of the Vegetation Fire on Backscattering: An Investigation Based on Sentinel-1 Observations

Pasquale Imperatore, *Member, IEEE*, Ramin Azar, Fabiana Calò, Daniela Stroppiana, *Member, IEEE*, Pietro Alessandro Brivio, *Senior Member, IEEE*, Riccardo Lanari, *Fellow, IEEE*, and Antonio Pepe, *Member, IEEE*

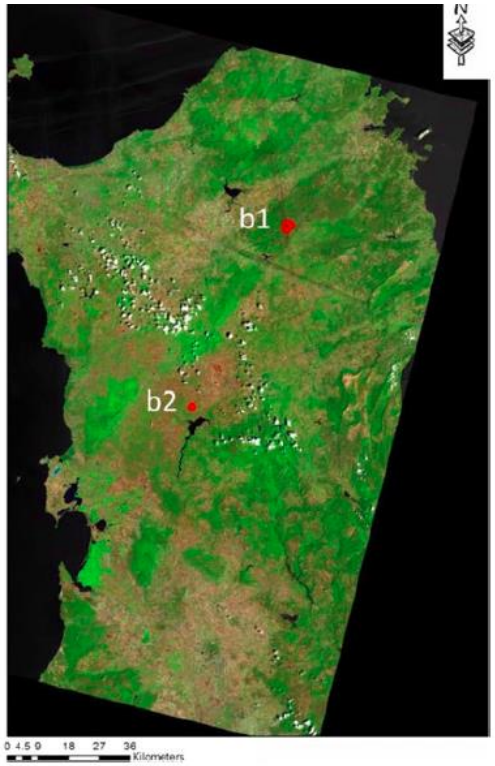

Fig. 2. Perimeters of the investigated burned areas, b1 and b2, (in red), superimposed on a Landat-8 OLI image (acquired on June 13, 2015).

Integration of SAR and Optical Data

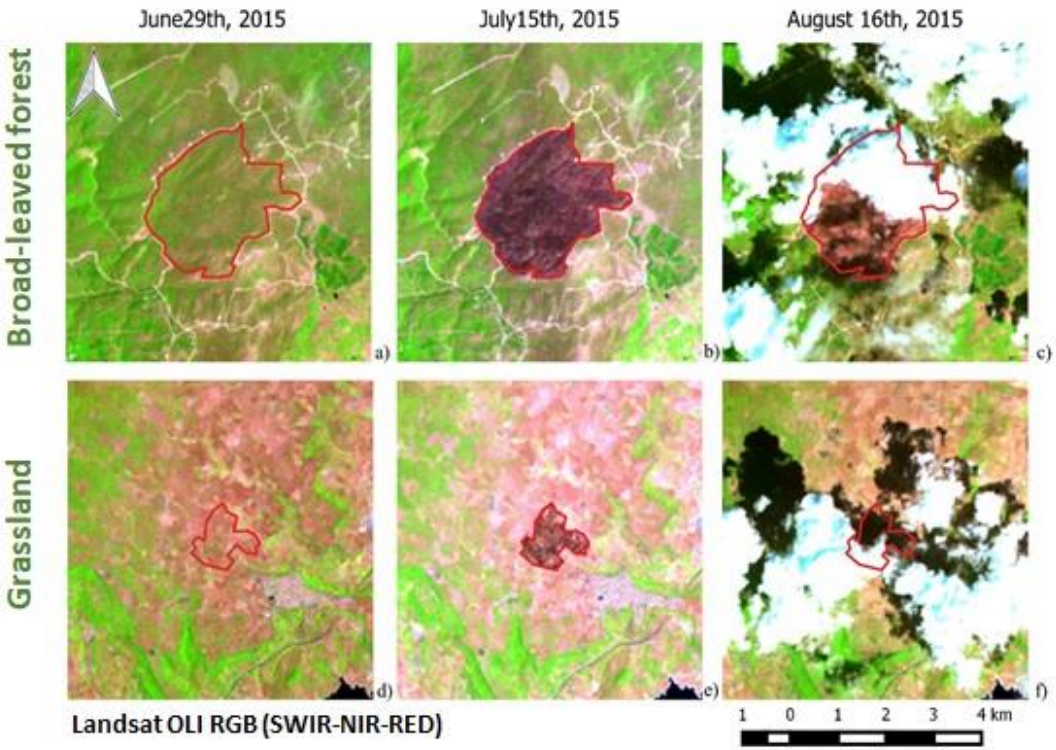

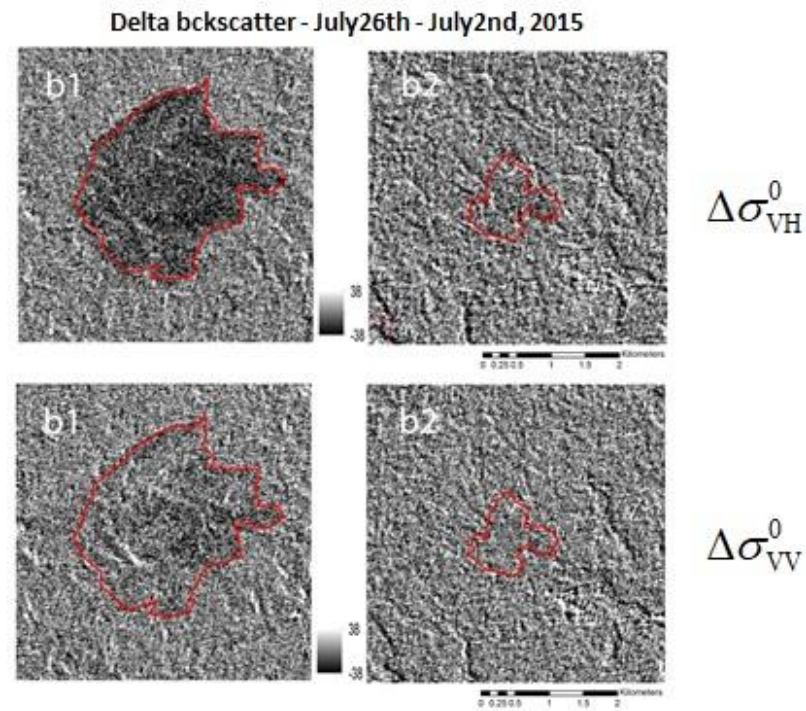

- The largest fire-disturbed area (b1) covers approximately 546 ha of forest vegetation near the town of *Budduso'* (Olbia-Tempio): the fire-event occurred on July 6, 2015.
- S1 Cross-polar (VH) amplitude information has successfully been used for burned area detection.

Integration of SAR and Optical Data

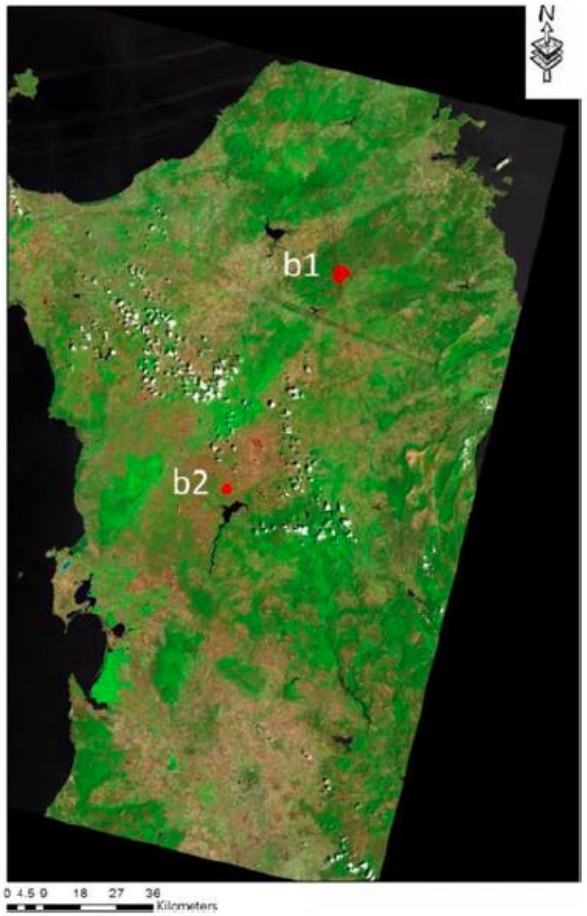

Fig. 2. Perimeters of the investigated burned areas, b1 and b2, (in red), superimposed on a Landat-8 OLI image (acquired on June 13, 2015).

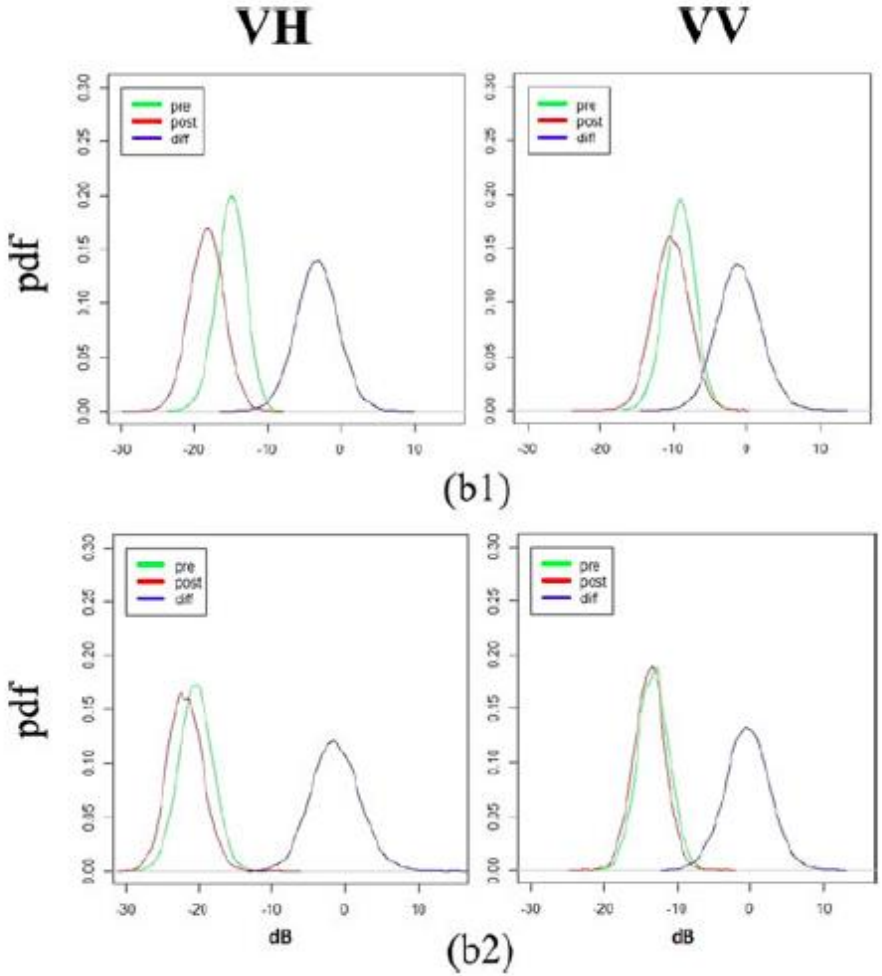

Fig. 8. Histograms of σ^0_{VH} and σ^0_{VV} pertinent to the different fire scars, b1 and b2, and before (green line) and after (red line) the fire event. The relevant $\Delta\sigma^0_{VH}$ and $\Delta\sigma^0_{VV}$ distributions are also shown (blue line).

Map of burned areas (Mt. Vesuvius)

Map of burned areas (Mt. Vesuvius)

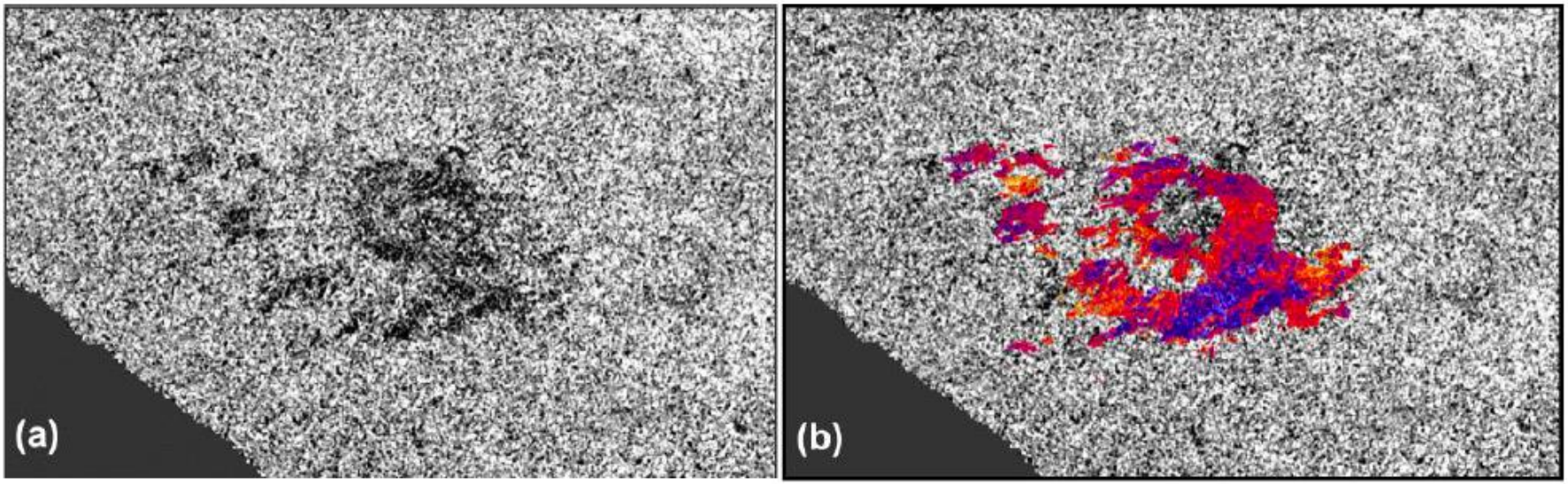

Figura 3. (a) Log-Ratio map of the May-September S-1 radiometrically calibrated SAR images. (b) Comparison between the map and the burned areas as derived from the Copenicus Emergency Management system catalogue.

June 12, 2017 – September 16, 2017 Sigma Nought Difference